Sedimentology (2008) **55**, 1419–1447 doi: 10.1111/j.1365-3091.2008.00951.x

Interplay between tectonics and compaction in a rift-margin, lacustrine delta system: Miocene of the Eger Graben, Czech Republic

MICHAL RAJCHL*†, DAVID ULIČNÝ‡ and KAREL MACH§
**Czech Geological Survey, Klárov 131/3, 118 21 Praha 1, Czech Republic (E-mail: michal.rajchl@geology.cz)*
†Institute of Geology and Palaeontology, Charles University, Albertov 6, 128 43 Praha 2, Czech Republic
‡Geophysical Institute, Czech Academy of Sciences, Boční II/1401, 141 31 Praha 4, Czech Republic
§Severočeské doly, a.s., Doly Bílina, 5 května 213, 418 29 Bílina, Czech Republic

ABSTRACT

The Early Miocene Bílina Palaeodelta consists of fluvio-deltaic and lacustrine clastics deposited along the south-eastern margin of the extensional Most Basin, part of the Eger Graben in north Bohemia (Czech Republic). The Bílina succession shows evidence of repeated advances of an axial deltaic system across a thick accumulation of organic material and clay in the hangingwall of an active fault. Exposures up to *ca* 4·5 km long in the Bílina open-cast mine help bridge the gap between seismic scale and typical outcrop scale of observation and thus allow the relationships between small-scale and basin-scale stratal geometries to be evaluated. The Bílina Palaeodelta deposits include sand-dominated, fluvial channel fills and heterolithic sheets interpreted as delta plain strata, sand-dominated mouth-bar wedges and heterolithic sheets of prodeltaic deposits, passing distally into lacustrine clays. The depositional environment is interpreted as a fluvial-dominated, mixed-load, lacustrine delta with a high degree of grain-size segregation at the feeder-channel mouths. On the largest temporal and spatial scales, variable tectonic subsidence controlled the overall advance and retreat of the delta system. The medium-term transgressive-regressive history was probably driven by episodes of increased subsidence rate. However, at this temporal scale, the architecture of the deltaic sequences (deltaic lobes and correlative lacustrine deposits) was strongly affected by: (i) compaction of underlying peat and clay which drove lateral offset stacking of medium-term sequences; and (ii) growth of a fault-propagation fold close to the active Bílina Fault. At the smallest scale, the geometries of individual mouth bars and groups of mouth bars (short-term sequences) reflect the interaction among sediment loading, compaction and growth faulting that produced high-frequency relative lake-level fluctuations and created local accommodation at the delta front.

Keywords Compaction, delta, Eger Graben, extensional tectonics, forced folding, growth fault, Miocene.

INTRODUCTION

The stratigraphic geometry of depositional systems is generally thought to reflect the interplay of subsidence, base-level changes and sediment supply (e.g. Van Wagoner *et al.*, 1990). Subsidence of the basin floor is primarily due to tectonic processes but it can be significantly modified by migration of ductile substrates, such as salt or overpressured clay, and by differential compaction. In systems with compressible and mobile substrates, the interaction among deposition, loading, compaction and/or interstratal remobilization can produce local accommodation that controls the resulting stratal geometries (e.g. Gay, 1989; Reynolds *et al.*, 1991; Howell *et al.*, 1996; Hunt *et al.*, 1996). In coal-bearing basins, syndepositional compaction of peat plays a significant, but as yet not fully explored, role in the depositional evolution and the resulting stratigraphic geometries (Ryer & Langer, 1980; Elliott, 1985; Flores & Pillmore, 1987; Diessel, 1992; Nadon, 1998; Michaelsen *et al.*, 2000).

The Miocene Bílina Palaeodelta is an important coarse-grained depositional system in the extensional Most Basin, the largest sub-basin of the Cenozoic Eger Graben of Central Europe (Fig. 1). An extensive lignite seam immediately underlies the Bílina deltaic succession (Figs 1B and 2). Evidence presented below shows that an axial delta system repeatedly advanced across a thick accumulation of organic material in the hanging-

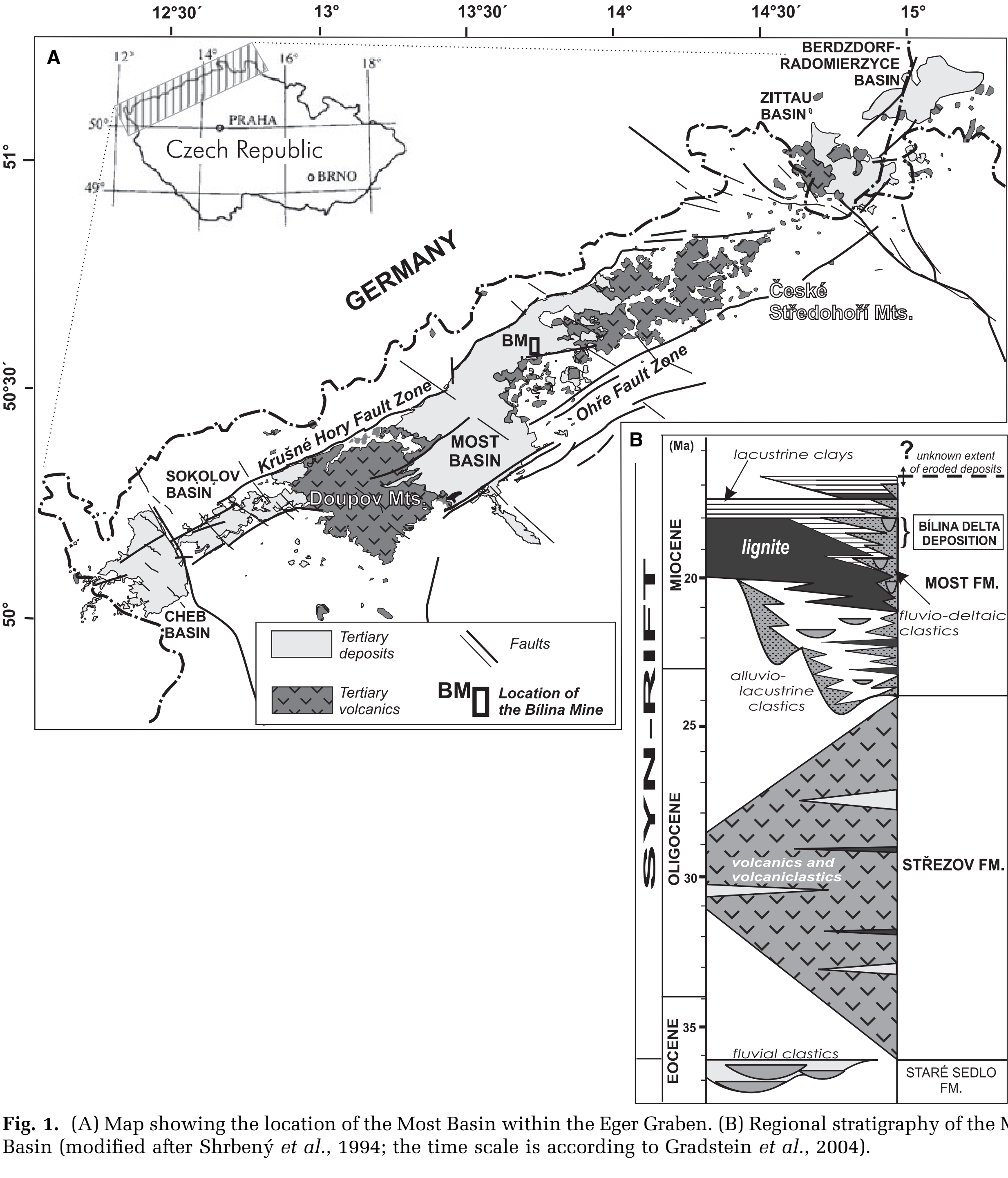

Fig. 1. (A) Map showing the location of the Most Basin within the Eger Graben. (B) Regional stratigraphy of the Most Basin (modified after Shrbený *et al.*, 1994; the time scale is according to Gradstein *et al.*, 2004).

wall of a normal fault that was active during deposition (Fig. 3). The size of the Bílina open-cast mine (over 4·5 km of continuous lateral exposure) bridges the gap between a typical outcrop scale and a seismic scale (cf. Fig. 2A). The continuous highwalls expose nearly the entire depositional system, along roughly one half of the width of the receiving graben, together with the underlying lignite, parts of pre-Cenozoic basement and also faults of regional importance. All these features make the Bílina Palaeodelta an attractive case for assessing the relative roles of tectonics and other controls in the formation of the exposed deltaic geometries, and potentially a useful outcrop analogue for lacustrine-deltaic hydrocarbon reservoirs.

The main aim of this paper was to document the interplay between tectonic fault-controlled subsidence, local accommodation associated with both shale and peat compaction, relative lake-level fluctuations at a variety of spatial and temporal scales, and the pattern of delta progradation. The interpretations presented below are of a qualitative nature, largely because of problems with accurate dating and estimating the rates of depositional processes (see below). However, the results provide useful insight into the wider role of compaction in controlling stratigraphic geometries in deltaic settings.

GEOLOGICAL SETTING

The Most Basin is one of five sub-basins preserved in the Eger Graben (the Ohře Graben or the Ohře Rift in other Czech literature). The sub-basins are separated from one another by volcanic highs and fault systems that cut the axis of the Eger Graben at a high angle (Fig. 1A).

Deposition in the Most Basin, and probably over the entire Eger Graben, took place approximately from the latest Eocene to the latest Early Miocene (Fig. 1) based on the geochronology of the associated volcanics (Adamovič & Coubal, 1999; Cajz *et al.*, 1999; Cajz, 2000) and palaeobotanical data (Kvaček, 1998) correlated with the Geological Time Scale (GTS) 2004 (Gradstein *et al.*, 2004). Limited biostratigraphical resolution means that the duration of nested stratigraphic cycles preserved in the Bílina Palaeodelta cannot be constrained. On the longest time scale, two extensional phases are interpreted as having controlled the subsidence rate and basin geometry (Rajchl, 2006). The first phase was characterized by NNE-SSW to N-S-oriented horizontal extension, oblique to the rift axis; this extension caused the formation of an E-W to ENE-WSW fault system (Rajchl & Uličný, 2000a; Špičáková *et al.*, 2000; Rajchl, 2006). This fault system created a number of depocentres associated with relatively low subsidence rates (Rajchl, 2006). The E-W fault segments were arranged in an en echelon pattern and were probably linked by relay ramps that locally served as entry points for clastic input (Fig. 3; Rajchl & Uličný, 2000a; cf. Gawthorpe *et al.*, 1994; Peacock & Sanderson, 1994). The second phase of extension, with the extension vector orthogonal to the rift axis, produced a NE-SW-trending fault system that overprinted the earlier structural fabric (Rajchl, 2006; cf. Špičáková *et al.*, 2000). Rajchl (2006) suggested that the youngest parts of the Bílina Palaeodelta could have been affected by the change in the extension direction, but the exact timing of the change in extension vectors is unclear. The Bílina Palaeodelta prograded along one of the Bílina Fault E-W segments, suggesting that its deposition took place during the first extensional phase.

The Bílina Palaeodelta is a unit of fluvio-deltaic clastics overlying an extensive lignite seam that is *ca* 30 m thick. The deltaic clastics were deposited locally along the south-eastern margin of the Most Basin, where a fluvial system entered a lacustrine environment enclosed within an extensive peat swamp during the Early Miocene (e.g. Hurník, 1959; Mach, 1997). This depositional system is relatively small (*ca* 5 km across), up to 150 m thick and is very well-exposed because of continuous excavation in the Bílina open-cast lignite mine. The margin of the preserved Bílina Palaeodelta deposits is cut by a segment of the Bílina Fault (Fig. 2A). Because of the partial erosion of the depositional record at the margins of the basin, and because of later reactivation of the fault systems (Rajchl, 2006), it is difficult to identify the actual fault segments that governed the subsidence of the Bílina depocentre. Figure 3 shows the synsedimentary fault pattern interpreted for the period of peat accumulation and the Bílina Palaeodelta activity based on isopach maps, interpretation of seismic reflection data, and stratal geometries in outcrop and the subsurface (Rajchl, 2006).

METHODS

The deltaic deposits in the Bílina open-cast mine have been studied using a combination of

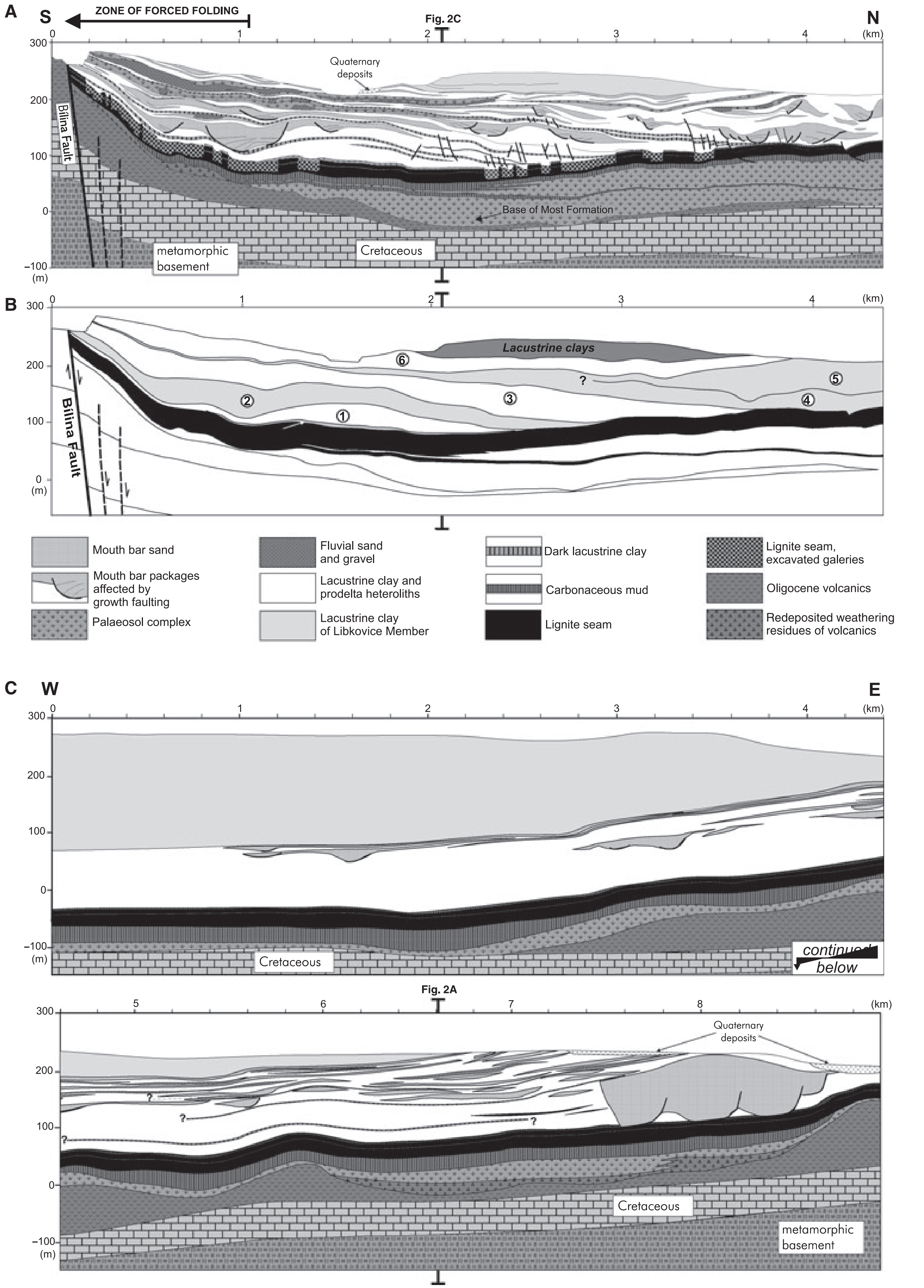

A
S
ZONE OF FORCED FOLDING
Fig. 2C
N
(km)
Quaternary deposits
Bílina Fault
Base of Most Formation
metamorphic basement
Cretaceous
(m)
B
Lacustrine clays
Bílina Fault
Mouth bar sand
Mouth bar packages affected by growth faulting
Palaeosol complex
Fluvial sand and gravel
Lacustrine clay and prodelta heteroliths
Lacustrine clay of Libkovice Member
Dark lacustrine clay
Carbonaceous mud
Lignite seam
Lignite seam, excavated galeries
Oligocene volcanics
Redeposited weathering residues of volcanics
C
W
E
Cretaceous
continued below
Fig. 2A
Quaternary deposits
Cretaceous
metamorphic basement

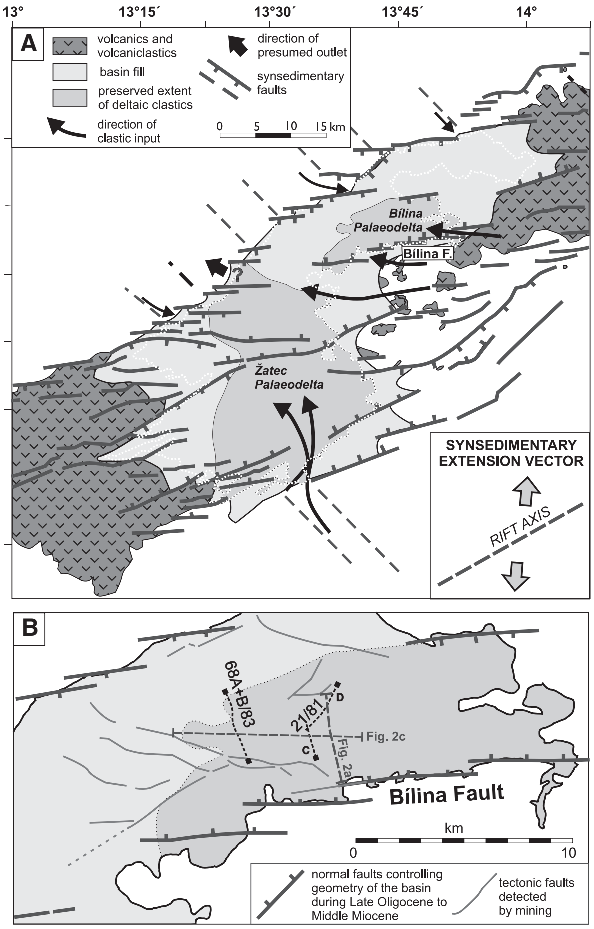

Fig. 3. (A) Interpreted palaeography for the period of peat accumulation and deposition of the Bílina Palaeodelta (modified after Rajchl, 2006). (B) Schematic location map showing position of the Bílina Palaeodelta within the Most Basin, the locations of the cross-sections shown in Fig. 2, and the reflection seismic profiles shown in Fig. 4.

photomosaics covering most of the lateral extent of the highwalls, and vertical sedimentological logging (Rajchl & Uličný, 1999). The larger scale geometry of the system was based on the interpretation of vertical two-dimensional cross-sections (Fig. 2) constructed from outcrop documentation of successive positions of highwalls of the Bílina mine between 1981 and 1996 (Dvořák & Mach, 1999). General orientation of all documented highwalls is transverse to the main depositional dip. Therefore, the cross-sectional dimensions of sedimentary bodies discussed here are derived from their lateral extent in the highwalls, roughly transverse to palaeoflow. Spatial reconstructions of geometries of selected architectural elements (e.g. mouth bars, channel fills) are based on correlation of several hundred cored boreholes (original data in Mach, 2003). Archive reflection seismic profiles 21/81 and 68/83, acquired in the early 1980s (Jihlavec & Novák, 1986), were recently reprocessed and reinterpreted (Rajchl *et al.*, 2003a,b; Fig. 4). These: (i) provide more precise information on the three-dimensional geometry of the delta deposits identified in outcrops; and (ii) constrain the spatial and temporal relationship between palaeoenvironments and the structural framework.

LITHOFACIES AND DEPOSITIONAL GEOMETRIES

The Bílina deltaic succession shows a hierarchical arrangement of depositional geometries (architectural elements *sensu* Miall, 1985, 1988, 1991) ranging in length scale from tens of metres to kilometres (Fig. 5). The small-scale architectural elements are represented by a number of distinctive lithofacies associations: (i) delta-plain heterolithic sheets; (ii) fluvial-channel fills; (iii) sand-dominated mouth-bar wedges; (iv) prodelta heterolithic sheets; and (v) lacustrine clay sheets (Figs 5 and 6). At an intermediate scale, these facies associations combine to form lenticular packages of fluvio-deltaic deposits, and tabular packages of lacustrine clay (Fig. 5). The largest architectural scale is represented by the complete assembly of deltaic and lacustrine deposits that comprises the Bílina Palaeodelta (Fig. 2). Its internal architecture is characterized by a shingle-like arrangement of deltaic and lacustrine deposits of systematically smaller scale.

The small-scale architectural elements, equivalent to facies associations (Bridge, 1993), record short-term physical processes (cf. Miall, 1991) and thus provide a basis for understanding the nature of the depositional system, and for establishing a facies model of the Bílina Palaeodelta. The medium-scale and large-scale architectures record the evolution of the palaeodelta at the depositional system and basinal scale, respec-

Fig. 2. (A) Cross-section of the part of the Bílina Palaeodelta depositional system exposed in the Bílina open-cast mine based on field documentation (modified after Dvořák & Mach, 1999). For location see Fig. 3B. (B) Six medium-term sequences that are recognized in the cross-section (A) above (for details see text and Fig. 15). (C) Cross-section of the part of the Bílina Palaeodelta depositional system, oriented parallel to the general direction of the delta progradation. The cross-section is based on correlation of borehole data. For location see Fig. 3B.

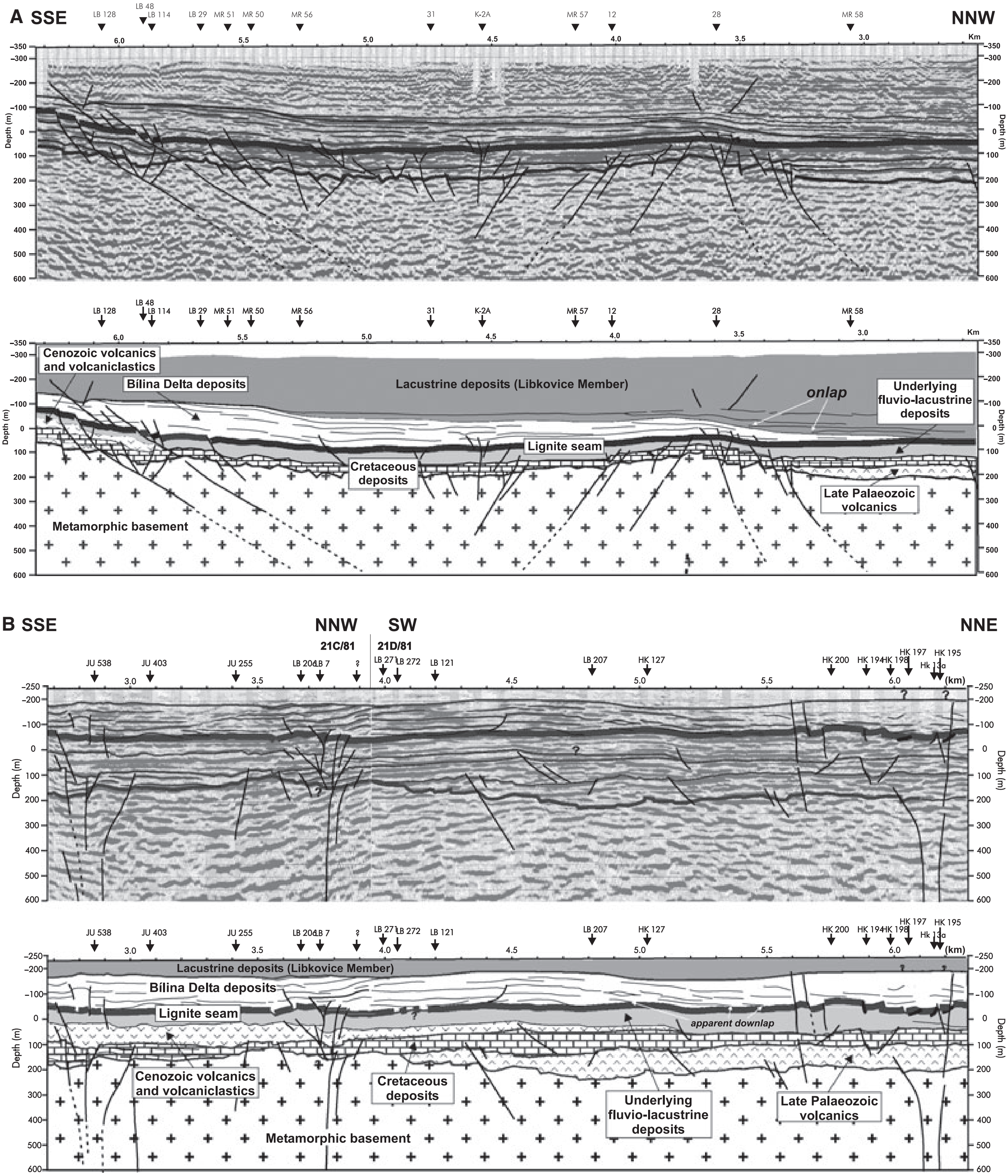

Fig. 4. Two examples of reflection seismic profiles 21/81 and 68/83 recently reprocessed and reinterpreted (Rajchl *et al.*, 2003a,b) and showing the geometry and architecture of the Bílina deltaic succession: for location, see Fig. 3B. (A) Profile 68/83 shows the distal part of the Bílina succession that is composed mostly of prodelta and lacustrine fines. This profile demonstrates the wedge shape and lateral northern pinchout of the Bílina Palaeodelta. Onlap of lacustrine strata onto the surface of the Bílina Palaeodelta sedimentary body suggests gradual drowning of the deltaic sedimentary system. (B) Part of profile 21/81 showing the proximal part of the Bílina succession which is dominated by sandy mouth bars. The shingle-like architecture and apparent downlap of deltaic strata onto the surface of the coal seam is well-displayed and documents lateral migration of the deltaic system.

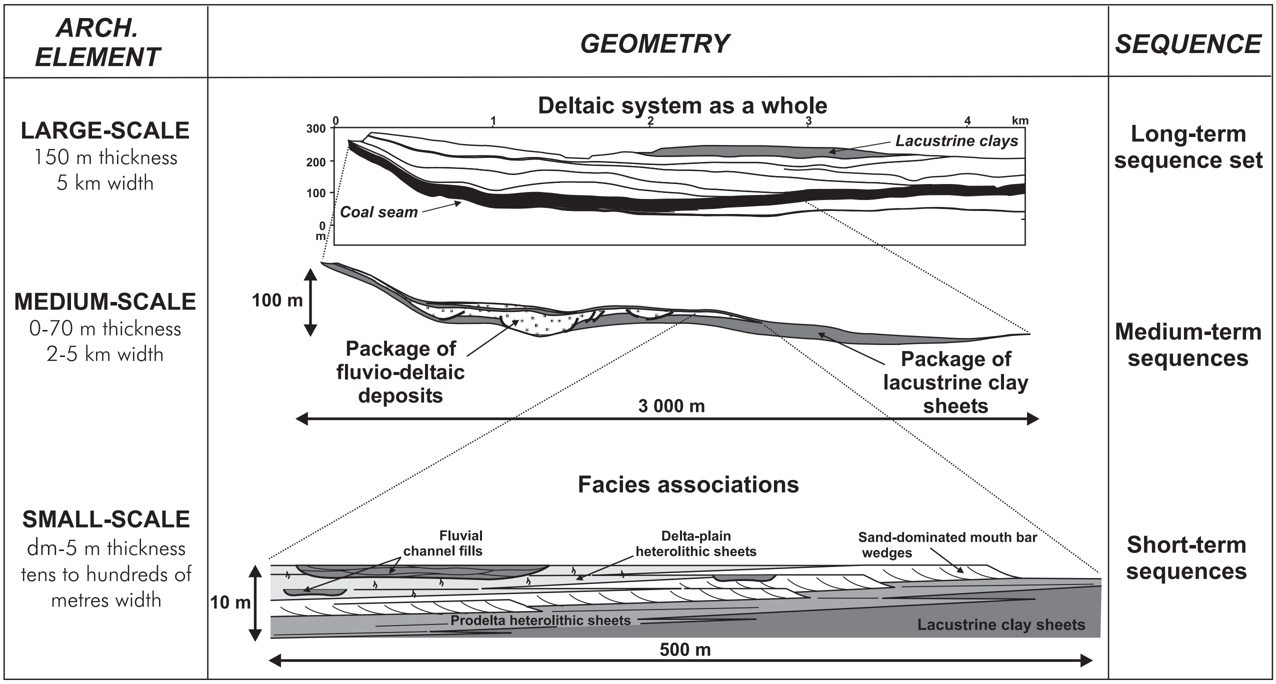

Fig. 5. Hierarchical arrangement of the main sedimentary geometries (architectural elements sensu Miall, 1985, 1991) and their sequence-stratigraphic interpretation.

tively, and provide data for understanding regional controls on the evolution of the delta. The descriptive part of the paper begins with a description and interpretation of the lithofacies associations followed by evaluation of the depositional geometries, presentation of a depositional model and, finally, by consideration of the sequence stratigraphic aspects.

Lithofacies associations: small-scale architectural elements

The spatial relationship between the facies associations that make up the deltaic system is shown schematically in Fig. 5. Component facies are summarized in Fig. 6. Each of the five associations is described and interpretations of depositional processes and palaeoenvironments are provided. The names of the architectural elements are based on a combination of their lithological and geometric characteristics and are partly interpretative for ease of further discussion and because the mutual geometric relationships in outcrop are generally straightforward. This section also includes a description and interpretation of the lignite seam.

Delta-plain heterolithic sheets are tens of centimetres to several metres thick and tens of metres to hundreds of metres wide. Three main lithofacies are distinguished: (i) *intensely rooted homogeneous deposits* (Fig. 7A) ranging in lithology from clay to sand; (ii) *carbonaceous mud* (Fig. 7B); (iii) *stratified sand to clay* (Fig. 7C), characterized by weakly rooted ripple cross-lamination, flaser bedding or lenticular lamination. Tree stumps, up to several metres tall, locally occur in (i) and (ii).

Interpretation: The *intensely rooted homogeneous deposits* are interpreted as palaeosols that developed on levées or in densely vegetated distal overbank deposits or distal crevasse splays; they dominate the delta plain record. The type of vegetation was a riparian forest characterized by a *Parrotia-Ulmus* association (Kvaček, 1998). The *carbonaceous mud* was deposited in areas of the swamp where the clastic input was low and marshes and peat bogs formed. The *stratified sand to clay* facies is interpreted as sparsely vegetated areas of the delta plain, as suggested by moderate rooting. It represents suspended load and bedload sediments deposited in areas beyond the reach of channellized flow. These sediments can represent deposits of interdistributary bays, crevasse splays or they may correspond to intervals of interruption of delta-plain deposition by a short-term rise in lake level.

Fluvial-channel fills are divided into two types according to scale: (i) *large-scale multi-storey and multi-lateral channel fills*, 50 m to several hun-

Arch. Elements	Lithofacies	Lithology	Sedimentary structures and other features	Sedimentary processes	Sedimentary environments
DELTA-PLAIN HETEROLITHIC SHEETS	Rooted homogeneous deposits	*Silty clay to silt, (clayey fine sand)*	*Homogeneous, rooted; tree stumps, slickensides*	*Intense pedogenesis*	*Palaeosols of delta-plain forests*
	Carbonaceous mud	*Dark clay rich in plant detritus, coal*	*Horizontal stratification, deformation by roots; tree stumps*	*Settling from suspension, plant detritus accumulation*	*Swamps of delta plain*
	Stratified sand to clay	*Silty clay to silt, clayey fine-grained sand*	*Laminae of sand, lenticular bedding, wavy bedding, wave ripples; deformation by roots can occur*	*Sedimentation from suspension alternating with tractional current*	*Interdistributary bays; interruptions of relative lake level rise*
FLUVIAL CHANNEL FILLS	LA sand	*Coarse-grained sand to fine-grained gravel*	*LA (lateral accretion) stratification, cross bedding*	*Lateral accretion*	*Active distributaries*
	Cross-bedded sand	*Fine-grained sand to fine-grained gravel*	*Trough cross-bedding, current ripples*	*Bedform migration*	*Active distributaries*
	Clay	*Silty clay to very fine-grained clayey sand*	*Planar stratification; U-shaped fill*	*Sedimentation from suspension*	*Abandoned distributaries*
SAND-DOMINATED MOUTH BAR WEDGES	Topset sand	*Medium to coarse grained sand*	*Trough cross-bedding, current ripples (locally climbing)*	*Bedform migration and aggradaion*	*Active subaqueous delta plain*
	Foreset sand	*Fine to medium grained sand*	*Inverse grading, homogeneous fabric*	*Grain flow, grainfall*	*Active delta front*
	Heterolithic interbeds	*Silty clay to silt, clayey very fine-grained sand*	*Flaser, wavy and lenticular lamination, laminae of sand draping planar stratification*	*Dominance of sedimentation from suspension*	*Subaqueous delta plain; delta front*
	Backset sand	*Fine to medium grained sand*	*Upslope-dipping cross-lamination, filling spoon-shaped scours*	*Upslope migration of hydraulic jump*	*Acive delta front*
	Homogeneous sands	*Fine to medium grained sand*	*Homogeneous fabric*	*Sliding and slumping on delta front*	*Delta front*
PRODELTA HETEROLITHIC SHEETS	Heteroliths	*Clayey fine grained sand to sandy clay to silty clay*	*Current and wave ripples, flaser bedding, wavy bedding, lenticular bedding, planar lamination*	*Sedimentation from density currents and suspension*	*Prodelta*
LACUSTRINE CLAY SHEETS	Clay	*Clay with varying admixture of silt*	*Planar lamination*	*Sedimentation from suspension*	*Lake*

Fig. 6. Overview of lithofacies and facies associations used to describe the fluvio-deltaic, lacustrine and swamp deposits.

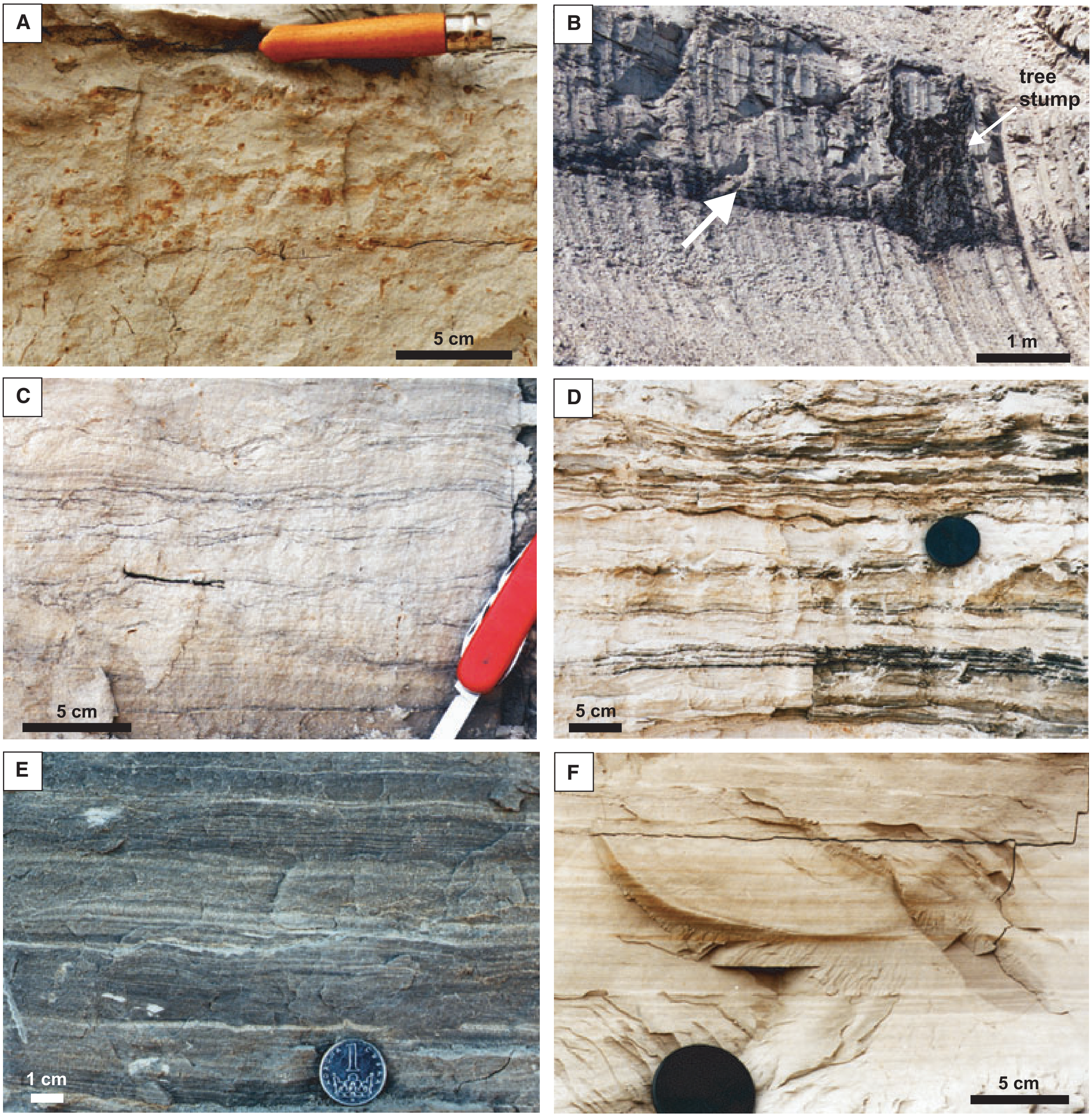

Fig. 7. (A) Intensely rooted homogeneous delta plain deposits. (B) Layer of carbonaceous mud (arrowed) with coalified tree stump. (C) Stratified sand to clay represented by flaser-bedded silty sand. (D) Thickly bedded heterolithic deposits of the proximal prodelta, layers of sand are ripple-bedded and mud layers are characterized by a high content of organic detritus. (E) Silt to silty clay of the distal prodelta, thinly interlaminated with fine-grained sand. (F) Thinly laminated lacustrine clay.

dred metres wide (maximum width 600 m) and 3 to 20 m thick, always consisting of a number of nested channel fills that are 5 to 30 m wide (Fig. 8A), and (ii) *isolated, small-scale channel fills,* 5 to 20 m wide and 0·5 to 1·5 m thick (Fig. 8B). The channel fills, mostly composed of coarse-grained sand to fine-grained gravel, commonly pass upwards into medium or fine-grained sand. The dominant sedimentary structures are trough cross-bedding with ripple-lamination in the upper parts of the channel fills. Lateral-accretion geometries occur only in the large-scale channel fills (Fig. 8A).

Interpretation: The large-scale channel fills, characterized by multi-storey and multi-lateral stacking, are interpreted as channel-belts formed

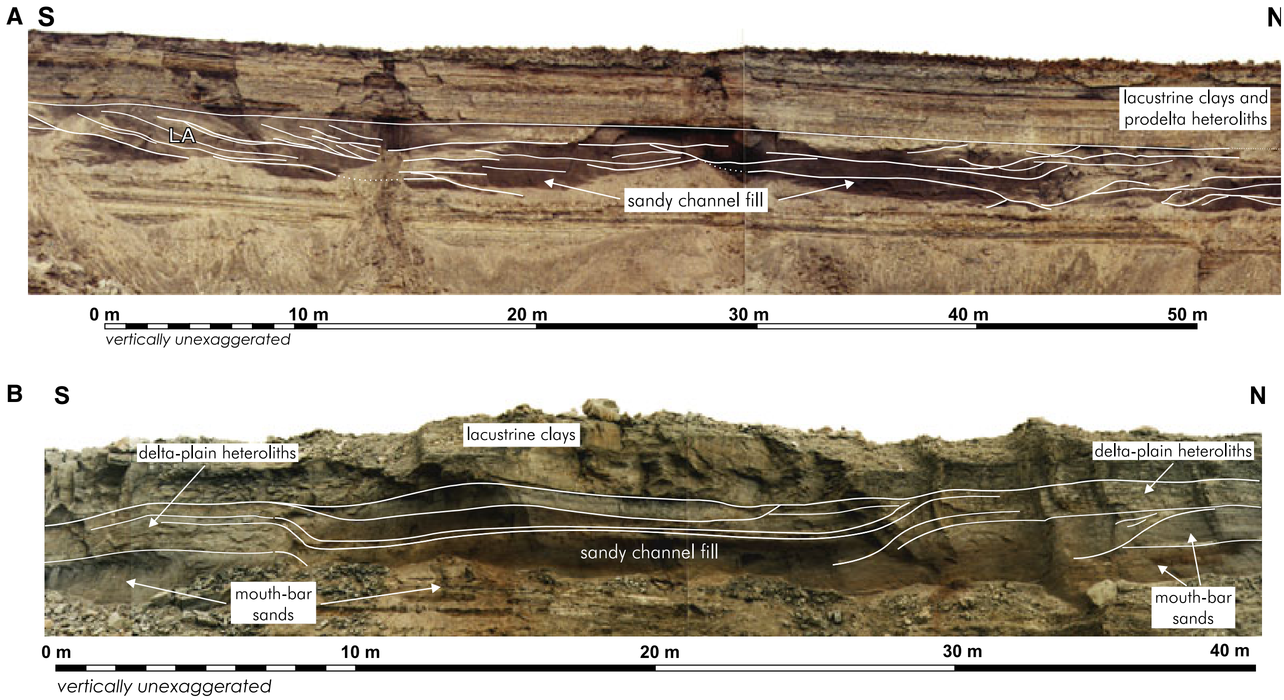

Fig. 8. (A) Part of large-scale channel fill characterized by multi-storey and multi-lateral stacking of individual subordinate channel fills, marked by white lines (LA – interpreted lateral accretion). (B) Group of small-scale channel fills incised into delta-plain deposits.

by lateral shifting of channels that were significantly narrower than the resulting channel belts (several tens of metres wide maximum). Channel deposition was dominated by sandy bedforms (dunes to ripples). The occurrence of lateral accretion surfaces and the high ratio between the channel-fill width and thickness suggests some degree of sinuosity (Miall, 1996). The isolated, small-scale channel fills are interpreted as distributaries that fed individual mouth bars. A lack of lateral-accretion geometries and a low spread of palaeocurrents indicate that these channels were relatively straight (*sensu* Bridge, 2003).

Sand-dominated mouth-bar wedges are up to 7 m thick and tens to several hundred metres wide (Figs 9 and 10); they are generally composed of fine to coarse-grained sand. The internal architecture of the mouth-bar wedges is characterized by originally flat-lying, trough cross-bedded or ripple-bedded topsets, and planar or tangential foresets, commonly steeply dipping (up to 30°) and typically with inversely graded laminae. Rarely, ripples migrated up the foreset slopes. The foresets commonly downlap sharply on the underlying prodelta heteroliths, but locally the fine-grained foresets pass tangentially into bottomsets (Figs 9 and 10A). Homogeneous sand bodies locally occur close to foreset toes, and backsets (*sensu* Nemec, 1990; Massari, 1996) filling erosional scars on foreset surfaces are common. The sandy topset and foreset strata are interbedded with centimetre-thick, silty or clayey layers that pass tangentially downdip into the prodelta heteroliths and commonly overlie the fine-grained foresets, which also tangentially pass into the prodelta heteroliths (see Fig. 10A; cf. 'interforesets' in Flores, 1990). In some cases, foresets are not developed and the mouth-bar bodies are represented by ripple-bedded or trough cross-bedded horizontal sheets of sand.

The architecture of the sand-dominated wedges is commonly affected by synsedimentary normal faults with listric fault planes (Fig. 11) that are characterized by a number of vertically stacked sandy wedges and significant aggradation of the topsets in the subsiding hangingwalls. These faults were transverse or slightly oblique to the direction of mouth-bar progradation. In other cases, divergence of stratal geometry is not related to listric faults (Fig. 12) and its causes are discussed further in the text.

Interpretation: The sand-dominated wedges are interpreted as friction-dominated mouth bars (cf. Wright, 1977; Bhattacharya & Walker, 1992;

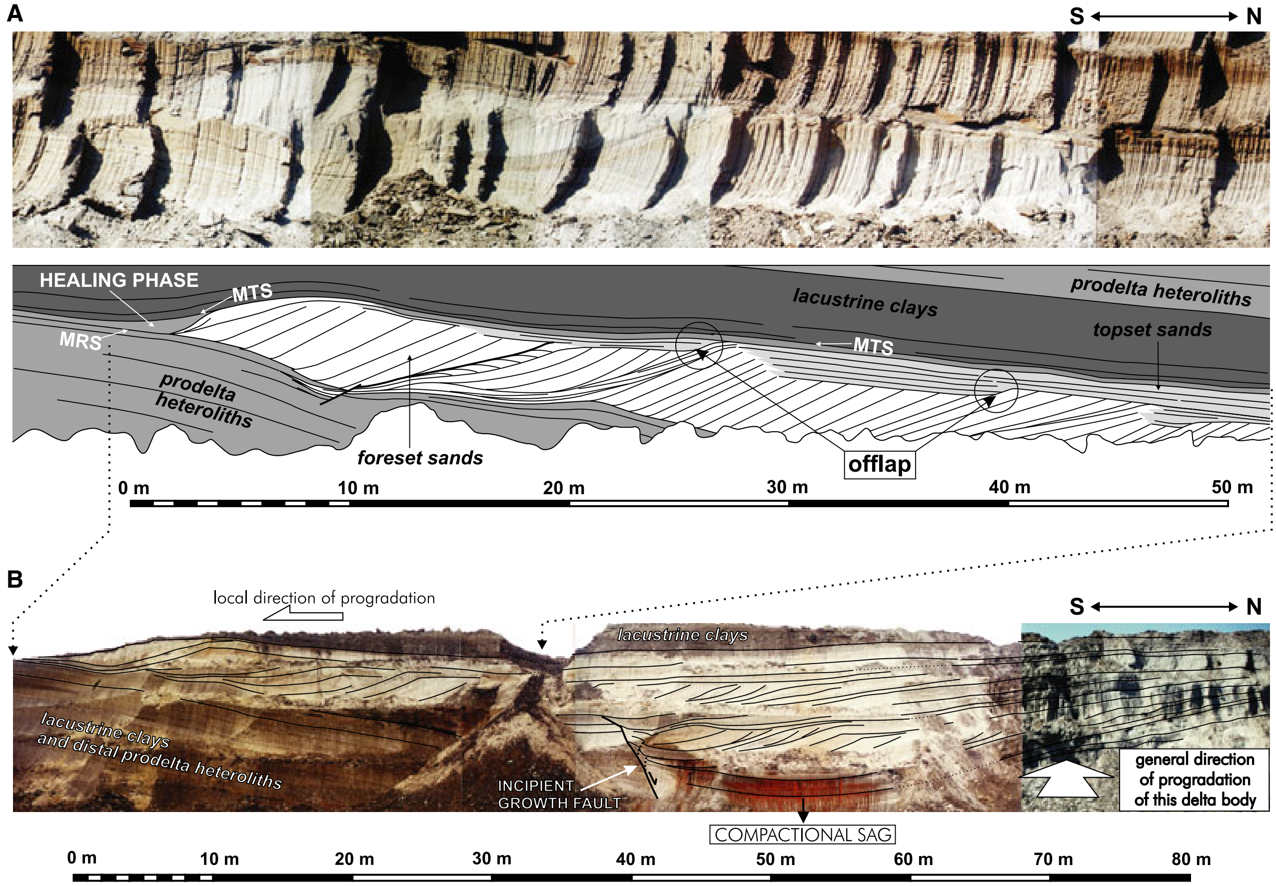

Fig. 9. (A) Example of a mouth bar with a Gilbert-type profile. Path of topset roll-over point in the mouth-bar architecture is an expression of relative lake-level change; offlapping foreset bodies suggest minor relative lake-level falls. Thin wedge of lacustrine clay, close to the mouth-bar face, is interpreted as a healing phase deposit and together with thin foreset beds, at the southern end of the mouth bar, represent the transgressive system tract of this sequence. (B) Group of mouth bars stacked in a compactional sag formed by loading of a thick package of lacustrine and prodelta deposits – note an incipient growth fault. After filling the available accommodation, the mouth bar prograded away from the sag area (the spatial distance between both pictures is several tens of metres). MRS–maximum regressive surface; MTS–maximum transgressive surface.

Postma, 1995, among many others). The mouth bars were typified mostly by a steep mouth-bar front dominated by grain-flow deposition, and characterized by a Gilbert-type profile (*sensu* Postma, 1990; Bhattacharya & Walker, 1992; Fig. 13A). The tangential geometry of some foresets could be caused by the erosional effect of a separation eddy which could also cause ripples to migrate up the foreset slope (Jopling, 1965). Locally, the mouth bars have a shoal-water profile (*sensu* Postma, 1990) in which the foresets are absent (Fig. 13B). The combined thickness of the mouth-bar foresets and sub-aqueous portion of the topsets is a rough measure of the water depth, typically not more than *ca* 2 to 5 m at the delta front. The shoal-water mouth bars formed in water depth of *ca* 1 m or less, although foreset beds of thickness less than 1 m also occur. The shallow depth led to frictional effects causing very rapid lateral expansion of the jets and a fan-like geometry of the mouth bars (cf. Allen, 1997).

The fine-grained sandy foresets and the fine-grained muddy layers interbedded with the foresets and topsets represent deceleration of the water flow and temporal inactivity of the mouth bars (cf. Flores, 1990). The foresets separated by these fine-grained interbeds are interpreted as having been deposited during individual high discharge events. The bodies of homogeneous sand, commonly occurring close to foreset toes, are attributed to collapse of unstable foreset deposits and downslope movement of grains as slumps or avalanches (*sensu* Nemec, 1990). The resulting scars were commonly filled by aggrading backset deposition, interpreted as resulting from hydraulic jumps formed above irregularities

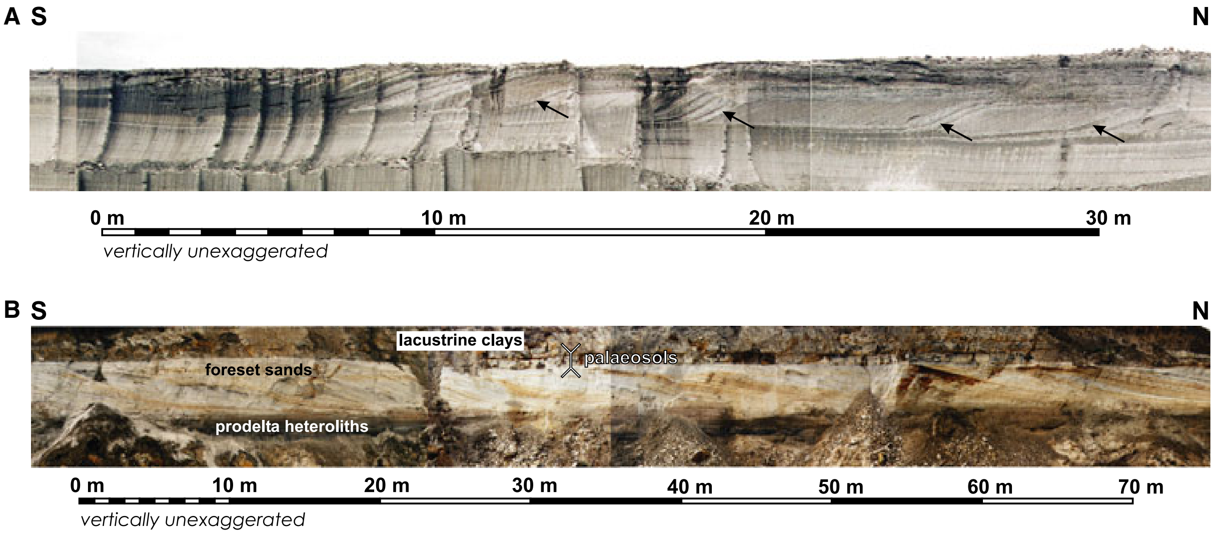

Fig. 10. (A) Photomosaic showing a mouth bar with a Gilbert-type profile: the southern part of the deltaic body shown in Fig. 11. The arrows show fine-grained and strongly aggradational intervals of the mouth bar, which were deposited during the later stage of the mouth-bar progradational phase. (B) Part of a laterally extensive mouth bar occurring in the uppermost part of the Bílina mine exposure. The mouth bar is characterized by an absence of topset facies coeval with the prograding foresets over the whole exposed length (several hundreds of metres) suggesting stillstand or a minor relative lake level fall during the progradation of this mouth bar.

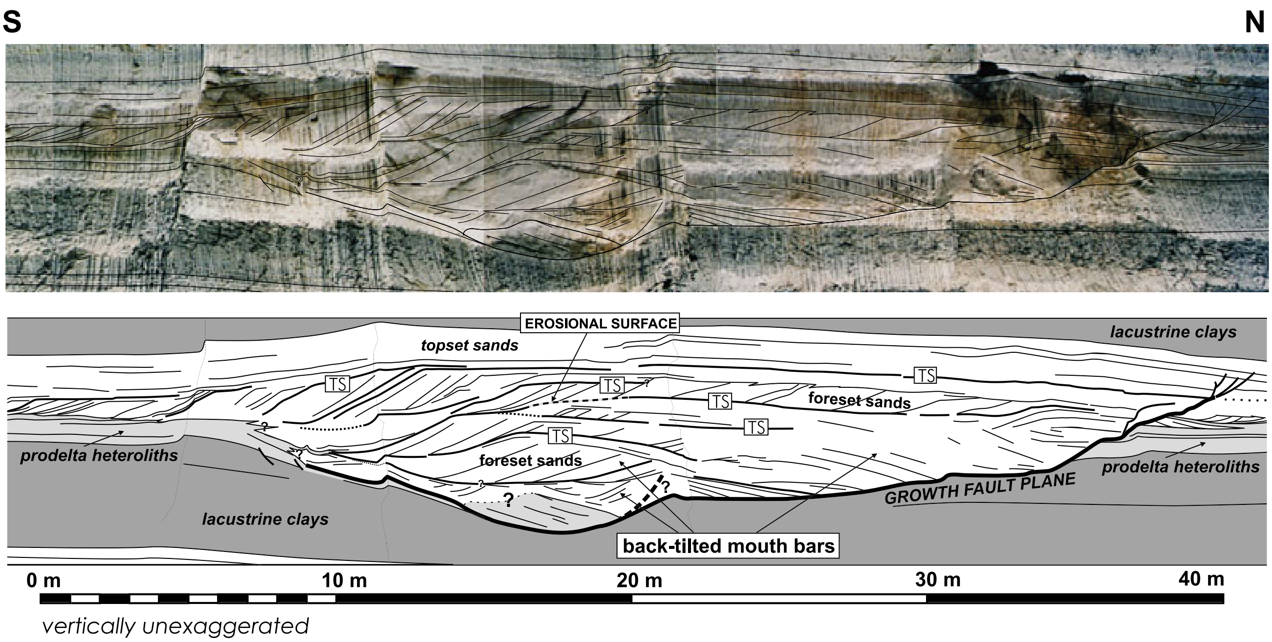

Fig. 11. Example of a deltaic body affected by growth faulting and characterized by systematic stacking of a number of mouth bars in the hangingwall. Note that several stacked mouth bars correspond to only a single mouth bar seen beyond the zone of the growth fault to the left and right of the photomosaic. The erosional surface in the middle of the section formed during uplift of part of the mouth bar, due to rollover anticline growth.

on the foreset face (*sensu* Nemec, 1990; Massari, 1996). Listric normal faults that affected the mouth-bar geometry are interpreted as growth faults (*sensu* Edwards, 1976; Nemec *et al.*, 1988) and have been described in the Bílina Palaeodelta by Rajchl (1999), Uličný *et al.* (2000), Rajchl & Uličný (2002) and Mach (2003).

Prodelta heterolithic sheets are up to 4 m thick and several hundred metres wide in cross-section, and commonly pass laterally up dip into

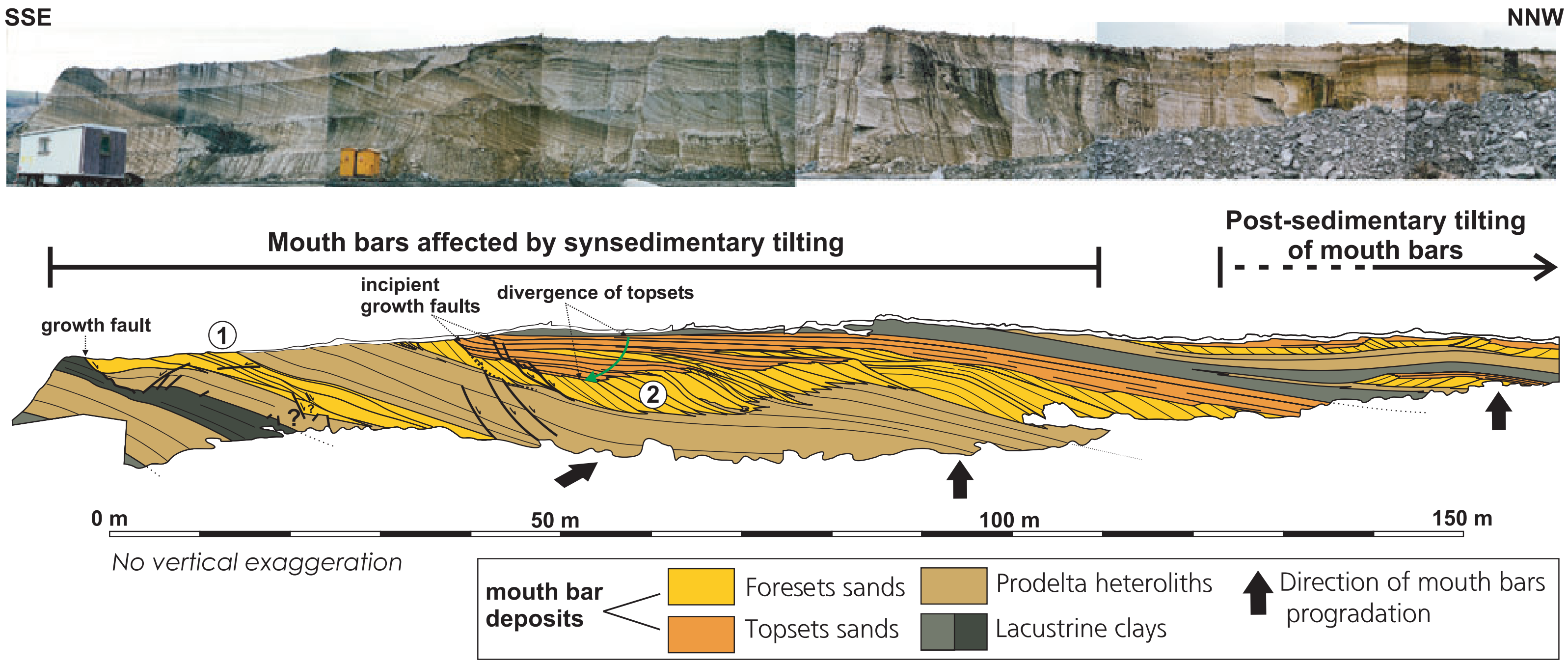

Fig. 12. Photomosaic and line drawing of a deltaic body showing significant divergence of stratal surfaces to the north (away from the Bílina Fault). Although minor growth faults occur in the succession, note that the strata diverge away from, not towards, the listric fault planes. These effects are interpreted as the consequence of synsedimentary tilting, shown most markedly in the fanning topset strata. Incipient growth faults suggest of a synsedimentary slope formed by the tilting. Successively deposited mouth-bar complexes are labelled (1) and (2) (see discussion in text).

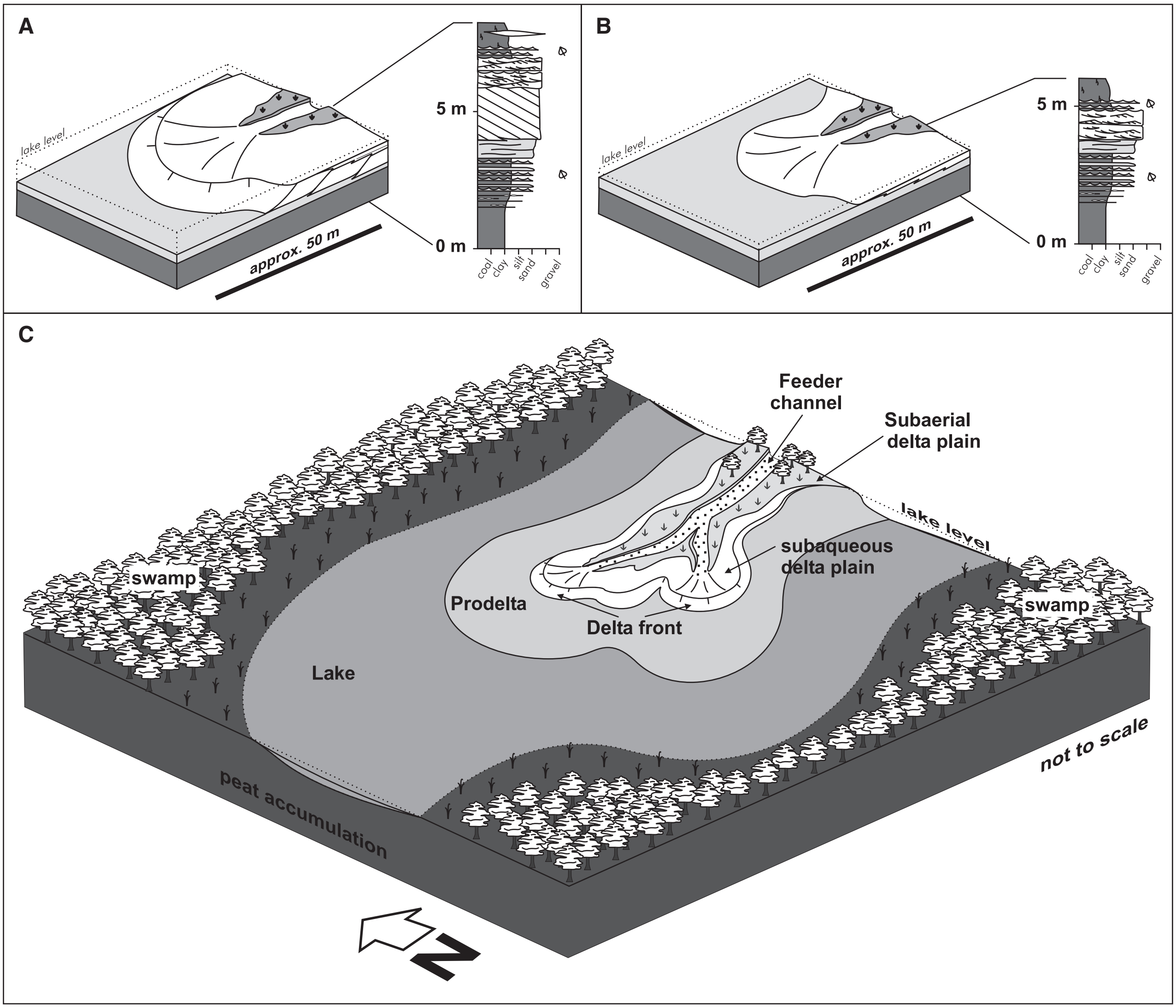

Fig. 13. Reconstruction of (A) Gilbert-type mouth bar and (B) mouth bar with shoal water profile. (C) Schematic 3D reconstruction of the Bílina Palaeodelta illustrating the relationship between the delta lacustrine environment and the surrounding swamp. The distance between the swamp edge and the delta lobes was several hundreds of metres to a few kilometres.

mouth-bar sand (Figs 9 and 10). Ripple-bedded or flaser-laminated fine-grained sand (Fig. 7D) dominate close to the mouth bars, whereas clay content increases distally. Distal prodelta heteroliths are characterized by interlaminated or lenticular laminated sand and silty clay (Fig. 7E). Laterally these deposits pass into the lacustrine clay sheets.

Interpretation: The continuity between mouth-bar foresets and the heterolithic sheets suggests that the latter are bottomsets of Gilbert-type mouth bars (or their genetic equivalents in case of shoal-water mouth bars). Current ripples and frequent alternation of the layers dominated by sand and clay could indicate deposition from density currents originating as hyperpycnal flows (e.g. Flores, 1990; Kostic *et al.*, 2002, and many others). A significant volume of the prodelta heteroliths grades laterally into the fine-grained layers separating the topsets and foresets (Figs 9 and 10A); this feature suggests coeval deposition on the delta front and prodelta during floods (cf. Flores, 1990).

Lacustrine clay sheets are thin (a few metres in thickness) sedimentary bodies that extend for hundreds of metres to kilometres. These sheets are formed by thinly laminated, light or dark brown clay with a varying admixture of silt (Fig. 7F). Laterally these deposits pass into the prodelta heteroliths. The boundary between prodelta and lacustrine deposits is defined by their content of sandy laminae, which are absent in the lacustrine deposits.

Interpretation: The lacustrine clays represent the finest grade material delivered to the basin by the feeder system and deposited furthest from the mouths of the distributaries. The organic matter content of the lacustrine clay, represented mainly by higher plant material, ranges between 1 and 5%, locally up to 9%. The dark colour of some sheets indicates a relatively lower quartz silt content and an increased organic carbon content. The lake is interpreted as fresh water, based on the observation of fresh water ostracod and gastropod fossils (Čtyroký & Witt, 1998), and also by the very low content of total organic-bound sulphur (0·38% to 2·07%, mean 0·89%, Mach *et al.*, 1999) in the lignite, especially in the upper part of the seam.

The **lignite seam** underlying the deltaic succession in the Bílina area is *ca* 30 m thick. The seam contains several thin interbeds of clay in the study locality, one of which is up to 2 m thick (Mach, 2002). According to Sýkorová *et al.* (1997), the bulk of lignite in the study area is characterized by a xylitic-detritic composition represented by macerals of huminite and liptinite groups, 15·7% average ash content, and reflectance (R_o) of 0·36.

Interpretation: According to Kvaček (1998) and Kvaček *et al.* (2004) the coal-forming vegetation represented a coniferous swamp forest dominated by *Glyptostrobus* and *Athrotaxis*. The presence of *Calamus, Sabal, Spirematospermum, Blechnum* and aquatic herbs *Stratiotes* and *Salvinia* documents a high groundwater level and frequent flooding of the swamp (Kvaček, 1998). The interbeds of clay also suggest frequent flooding of the swamp and subsequent interruption of the organic deposition by accumulation of fine-grained clastics.

Medium-scale architecture

The lithofacies associations are grouped into two types of medium-scale architectural elements: (i) *lenticular packages of fluvio-deltaic deposits*; and (ii) *packages of lacustrine clay sheets* (Fig. 5). These medium-scale architectural elements are arranged in successions separated from each other by prominent layers of dark lacustrine clay forming the basal part of the lacustrine clay sheets (Fig. 2A and B).

The **packages of fluvio-deltaic deposits** are characterized in cross-section by a flat lenticular or wedge-shaped geometry (Figs 2A and 9B). These bodies are commonly formed by several, laterally offlapping mouth-bar wedges and corresponding topset and bottomset strata (Fig. 9B). These bodies range in lateral extent from hundreds of metres to a few kilometres. Figure 5 shows an idealized arrangement of the individual architectural elements forming a deltaic body. The thickness of the bodies ranges from *ca* 3 m to several tens of metres (to a maximum of 70 m), with the thick examples affected by growth faulting (Fig. 11). Hangingwalls of the growth faults are characterized by multiple stacked mouth-bar wedges (Fig. 11; cf. Edwards, 1976; Nemec *et al.*, 1988; Morley & Guerin, 1996).

The **packages of lacustrine clay sheets** are composite bodies up to several tens of metres thick and extend laterally over several kilometres. In the distal parts of the deltaic system, these strata laterally interfinger with the uppermost part of the lignite seam as centimetre-thick interbeds of originally lacustrine clay that were subsequently rooted (Fig. 14; Mach, 2002, 2003). Each of the medium-scale packages of fluvio-deltaic clastics represents a grouping of individual mouth bars and closely associated deltaic facies, and the individual packages of lacustrine clay sheets represent their downdip equivalents.

Large-scale architecture

The entire Bílina deltaic succession forms a wedge-shaped body *ca* 5 km across in the N-S transverse cross-section (Figs 2A and 4A) and about 15 km long (in an E-W direction) parallel to the depositional dip. It reaches up to 150 m in thickness (Fig. 2). The lower bounding surface of this clastic body is characterized in transverse section by an apparent downlap of deltaic-lacustrine strata onto the top of the lignite seam (the role of compaction in creating the apparent downlap geometry is explained further below). Outcrop observations show that the interaction between the basal parts of the lacustrine-deltaic succession and the seam is more complex and includes partial interfingering of the lacustrine clays with the uppermost part of the seam (Fig. 14), or an occurrence of an interval of rooted clays with large tree stumps at the top of the seam. The upper limit of the Bílina deltaic succession body is defined by the base of the overlying lacustrine strata of the Libkovice Member (Fig. 2).

The internal architecture of this wedge is generally characterized by a shingle-like lateral arrangement of the medium-scale packages

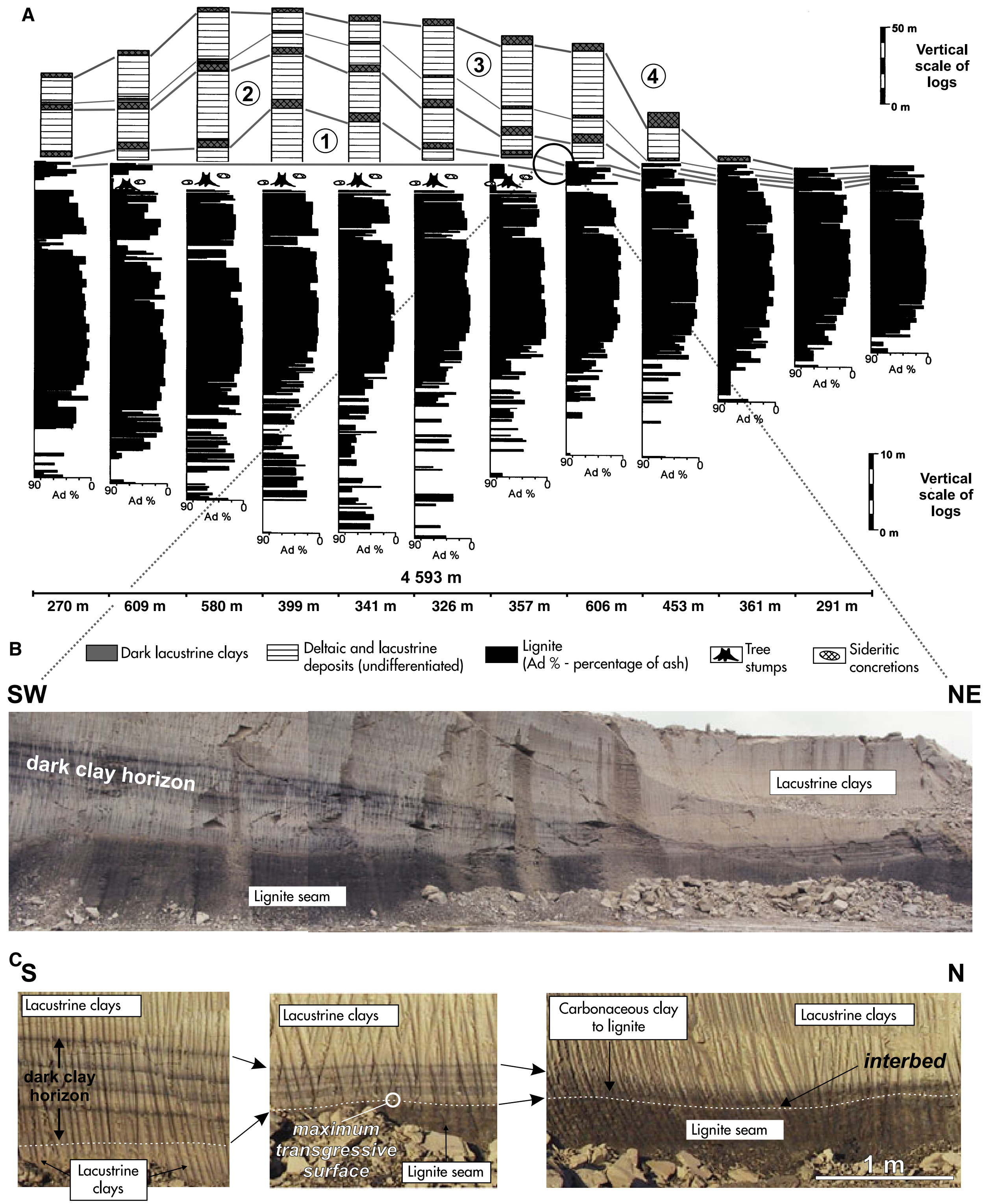

Fig. 14. (A) Correlation panel, based on borehole data from line of cross-section shown in Fig. 2A, showing the relationship between Bílina delta clastics and the lignite seam. Numbers 1 to 4 correspond to sequences 1 to 4 in Fig. 2B. Individual maximum transgressive surfaces, marked by horizons of dark clay, pass into the seam. (B and C) The photographs show apparent downlap of a dark clay horizon onto the seam. (C) Details from a 50 m long photomosaic (B) documenting correlation of a flooding surface that can be traced from deltaic deposits into the lignite seam.

described above (Fig. 2A) which, in seismic data, is expressed as oblique reflections downlapping against the lignite seam (Fig. 4). The sandy facies of the Bílina deltaic complex pinch out *ca* 6 km west of the Bílina Mine (Fig. 2C); the corresponding prodelta and lacustrine deposits extend more than 5 km further westwards. The well-log data show a progressive westward decrease in prevailing grain-size of the deltaic deposits. In seismic section 68/83, the deltaic wedge is represented predominantly by clay (Fig. 4A). The laterally offset stacking pattern of sedimentary bodies in both outcrop and seismic sections reflects a stepwise migration of the deltaic system towards the north (Figs 2A and 4B) in addition to overall progradation of the delta to the west as shown by well-log data (Mach, 2003; Fig. 2C).

SEDIMENTARY MODEL OF THE BÍLINA PALAEODELTA

The spatial extent and 3D reconstruction of the geometry of individual deltaic bodies show a distinctly lobate morphology (Fig. 13C). This geometry supports the interpretation of the Bílina Palaeodelta as a fluvial-dominated, mouth-bar-type delta with distributaries terminating in sandy Gilbert-type mouth bars. A significant feature of the Bílina Palaeodelta is the strong grain-size segregation between different delta environments. The delta plain and prodelta were dominated by muddy lithologies, with a subordinate proportion of heterolithic facies, whereas the feeder channels and mouth bars were dominated by sand. Homopycnal turbulent jets were probably the main type of effluent at the distributary mouths, consistent with a small difference in density between the waters of the fluvial feeder system and the fresh water of the lake. Turbulent mixing and friction at the distributary mouth led to rapid deceleration of the jet (cf. Allen, 1997) and the deposition of coarse material on the foresets. These effects were responsible for the pronounced grain-size segregation, as well as for the formation of Gilbert-type foresets (e.g. Postma, 1990). Only fine-grained suspended sediment reached the prodelta area.

The heterogeneous sediments of the Bílina Palaeodelta suggest that the fluvial system was characterized by a mixed sediment load. Individual channels within the large-scale channel belts are larger than the small-scale distributaries, suggesting downstream bifurcation of the channels – a typical feature of friction-dominated settings (Van Heerden & Roberts, 1988; Flint *et al.*, 1989). However, it is not possible to prove that several mouth bars were simultaneously active. The abundance and simple infill style of isolated, small-scale channel fills suggest that they were short-lived, possibly related to frequent avulsion (cf. e.g. Frazier, 1967; Törnqvist *et al.*, 1996). The muddy 'interforesets' within the mouth bars possibly reflect pauses in mouth-bar progradation caused by avulsions.

The receiving lake is interpreted as having been initially relatively small with respect to the whole basin (several square kilometres, Dvořák & Mach, 1999; Mach, 2003) and surrounded by peat swamp over most of the lifetime of the delta system. Previous studies (Malkovský, 1995; Suhr, 2003; Rajchl & Uličný, 2005) assume the lake to have been hydrologically open, with an outlet situated most likely opposite the Žatec 'delta' system (Fig. 3A).

SEQUENCE STRATIGRAPHY OF THE BÍLINA PALAEODELTA

The architecture of the Bílina Palaeodelta records a hierarchy of rapid to longer-term changes in depositional environment and water depth, which can be interpreted in a sequence-stratigraphic framework. In the Bílina Mine exposures, the most readily recognizable and correlatable surfaces of sequence-stratigraphic significance are surfaces of maximum (lacustrine) transgression. In contrast, sub-aerial unconformities ('Exxon-type' sequence boundaries *sensu* Van Wagoner *et al.*, 1988, 1990) are mostly not recognized. As a result, the sequences described below are genetic sequences (*sensu* Galloway, 1989).

The genetic sequence-stratigraphic interpretation of the architectural elements of the Bílina deltaic succession follows the hierarchy of the architectural elements. Three levels of genetic sequences are recognized (Fig. 5): the small-scale architectural elements correspond to highly localized, *short-term sequences*. These are grouped into *medium-term (composite) sequences*, recognizable over the whole deltaic system and, in several cases, traceable into the underlying lignite seam. The long-term depositional history of the Bílina Palaeodelta at the basinal scale represents a *long-term sequence set*.

Small-scale architecture: short-term sequences

Because of the lack of recognizable sub-aerial unconformities and sparse evidence for relative lake-level falls (see below), a simple two-fold division of sequences, into regressive systems tracts (RST) and transgressive systems tracts (TST), is used in the short-term sequences (cf. Helland-Hansen & Martinsen, 1996). The term 'systems tract' is used in the geometric sense of Swift *et al.* (1991) and Helland-Hansen & Martinsen (1996). A mouth-bar wedge with correlative landward and lakeward delta-plain, prodelta and lacustrine deposits represents a RST of a high-frequency sequence. In addition to a strongly progradational geometry, an aggradational geometry is also common, expressed in thick packages of topset and bottomset (prodelta) deposits. In the uppermost part of the Bílina deltaic succession, a laterally extensive mouth bar occurs without topset facies coeval with the prograding foresets (Fig. 10B). The offlapping geometry with an absence of topset strata over the exposed length (several hundred metres) of the mouth bar suggests the possibility of bypass of coarse clastics, because of stillstand or a minor relative lake-level fall during the progradation of this RST.

The TST is weakly developed relative to the RST. A TST is locally represented by backstepping, very thin mouth-bar wedges (Fig. 15) and/or by a thin wedge interpreted as a healing-phase deposit (Fig. 9). However, the transgressive phase is commonly represented only by a pronounced flooding surface defined by a sharp contact between the overlying lacustrine clays and the underlying sandy mouth-bar deposits. In this case the maximum regressive surface coincides with a maximum transgressive surface (*sensu* Helland-Hansen & Martinsen, 1996). The transgressive surfaces are commonly marked by a thin layer of scattered organic detritus, probably as a consequence of wave reworking. The lack of significant TST deposition is interpreted as reflecting lacustrine flooding of mouth bars almost immediately after their abandonment, presumably resulting from distributary channel avulsion (e.g. Frazier, 1967; Törnqvist *et al.*, 1996).

The internal geometry of the RST illustrated in Fig. 9 and the trajectory of the topset edge (i.e. rollover point) reveal a complex pattern of rapidly changing depositional geometries, progradation coupled with topset aggradation, short-term offlap and progradation with apparent bypass of the topset suggesting fluctuations in lake level at

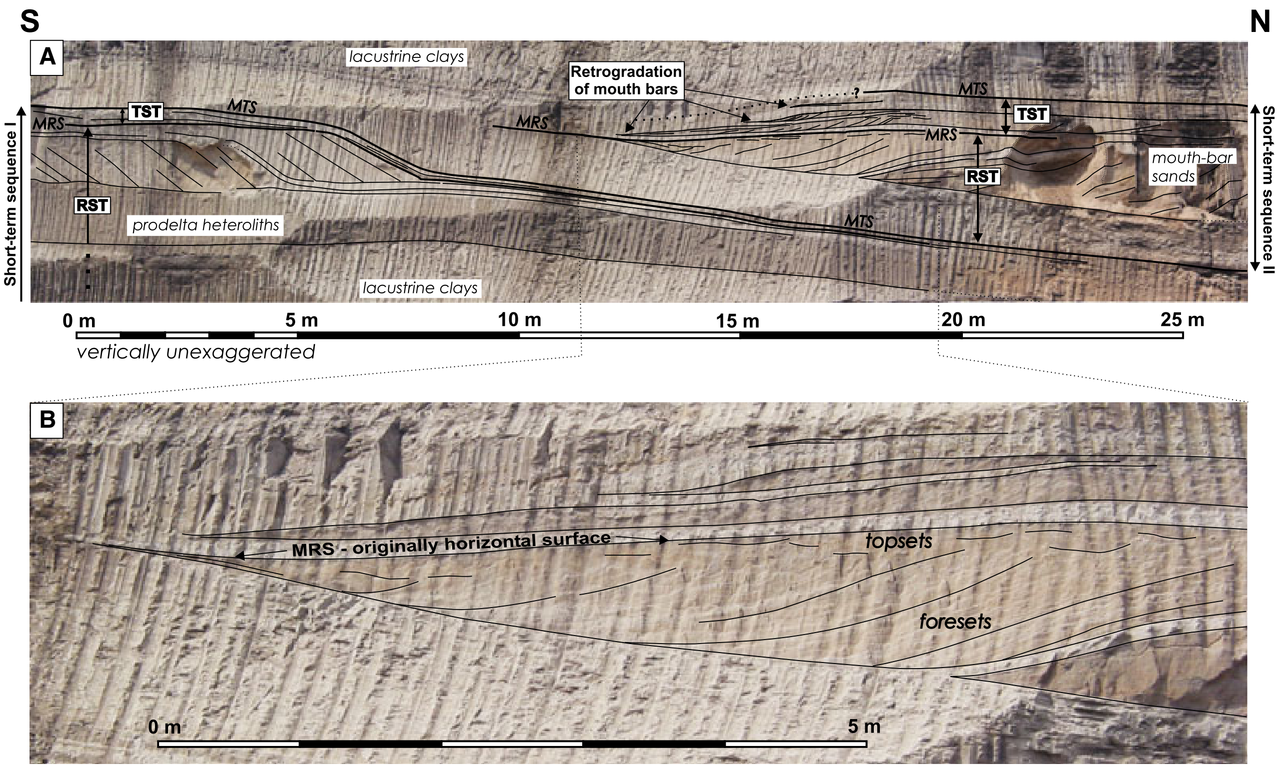

Fig. 15. (A) Example of two short-term sequences characterized by relatively thick RSTs compared to condensed TSTs. The TST of the younger sequence is represented by three retrograding very thin mouth bars. (B) The detail of the mouth bar on the right in (A) documents a significant role for sagging of the underlying clay during formation of accommodation for the mouth bar. Location of the lignite seam is several tens of metres below this mouth bar and peat compaction was not significant in this case. MRS–maximum regressive surface; MTS–maximum transgressive surface.

the scale of several tens of centimetres. Within this short-term RST, a number of 'parasequences' or sequences of yet smaller scale can be defined representing progradational increments of the foresets, separated by lacustrine mud-draped flooding surfaces or by several centimetres of offlap. A more detailed interpretation of such extremely short-term parasequences, which probably correspond to individual floods and/or localized compaction, is impossible because of the limited stratigraphic resolution provided by the 2D exposures. In general, there is very little evidence for relative lake-level fall.

Medium-scale architecture: medium-term sequences

Each of the medium-scale packages that represent individual delta lobes or whole deltaic bodies is interpreted as representing a single phase of delta progradation following a major lacustrine flooding episode. The most prominent flooding episodes were used to divide the Bílina deltaic succession into six composite, medium-term genetic sequences (Figs 2B and 16), typically composed of several tens of short-term sequences. Because the Bílina mine exposure provides only a limited view of the whole deltaic system, it is emphasized here that the six medium-term sequences represent only a partial record of delta evolution; in a cross-section located elsewhere a different number of sequences of the same order would probably be found.

The medium-term sequences show a typical vertical profile characterized by a shallowing upward (progradational) pattern: lacustrine and prodelta deposits dominate in the lower parts, whereas abundant floodplain strata, with palaeosols and channel fills, characterize the upper parts of the sequences (Fig. 2A). As in the case of the short-term sequences, it is difficult to find clear evidence of a significant relative lake-level fall and the formation of a sub-aerial unconformity. In several cases, channels are incised several metres

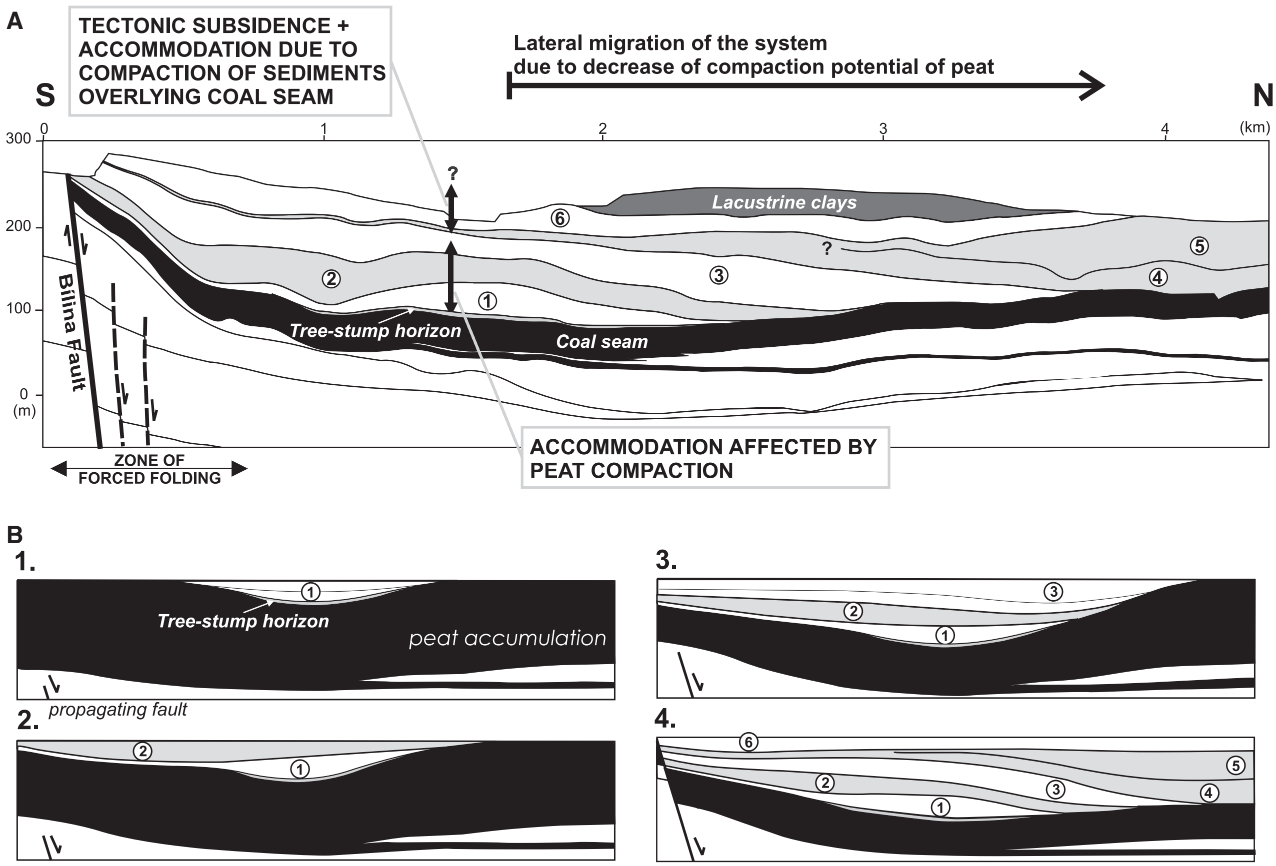

Fig. 16. (A) Distribution of the six medium-term sequences recognized in the Bílina Mine exposure. Geometry and stacking pattern of the sequences indicate a significant role for peat compaction during evolution of the deltaic system. (B) Conceptual model of evolution of stratal geometries of sequences 1 to 6 related to successive loading of the lignite seam, as exposed in the Bílina Mine. Note the onlap of younger sequences onto the surface of the seam reflects the gradual expansion of deltaic deposition to regions with sufficient compaction potential still available.

deep into mouth-bar deposits, but that does not exclude the possibility of the extension of a high-energy, deep distributary channel across the delta top (Fig. 17). In plan view, sandy equivalents of the individual medium-term sequences have a lobe-shape geometry (Fig. 18).

An important link between the evolution of the deltaic system and the peat swamp is the correlation of the dark clay horizons separating the medium-term sequences and the clayey interbeds in the lignite seam (Fig. 14; Mach, 2003). This interfingering relationship shows that the deltaic system did not really downlap onto a drowned peat bog flooded in a single step, but instead it originally *onlapped* on the margins of a coeval, actively growing peat swamp intermittently flooded by the lake, with organic growth temporarily suppressed and re-established. Subsequent compaction resulted in flattening of the seam surface leading to an apparent downlap geometry. The seismic resolution does not make it possible to distinguish the clayey interbeds. Figure 19 shows a qualitative model illustrating the response of the clastic lacustrine-deltaic system and the peat swamp to a cyclical change in lake level. In this interpretation, the dark lacustrine clays and the corresponding interbeds in the seam represent the early RST, recording incipient progradation of the deltaic system during a period of high relative lake level following flooding. The bulk of a typical medium-term sequence represents a composite RST. The TSTs of medium-term sequences are suppressed and, if present, are represented only by several centimetres of light-grey lacustrine clay. Generally the maximum transgressive surface coincides with the maximum regressive surface (*sensu* Helland-Hansen & Martinsen, 1996).

Sequence 1 (Figs 2B and 16) overlies the top of the lignite seam and, over a distance of *ca* 2 km (Fig. 14A), a prominent tree stump horizon that replaces the topmost parts of the seam in the central part of the Bílina mine. This interval of palaeosols with large stumps, developed in up to 6 m of clays (Fig. 14B), also contains a clay-dominated channel fill laterally passing into the rooted palaeosol clays (Fig. 20). This interval is not considered a part of the lacustrine-deltaic succession: instead, it is interpreted as a distal part of a fluvial system that carried suspended load into the peat swamp, in a way similar to that of the Hrabák fluvial system described from the Most Basin by Rajchl & Uličný (2005). The boundary between the rooted clays with stumps and the overlying, laminated, lacustrine clays, constitutes the base of sequence 1. This sequence is characterized by the absence of coarse-grained deltaic deposits in the study area and is represented only by a lenticular package of lacustrine clay in the Bílina section (Fig. 2A). The lateral extent of the sandy part of this sequence is shown in Fig. 18.

Sequences 2 and 3 are characterized by large deltaic bodies surrounded by relatively thick accumulations of lacustrine clay. Sequence 2 contains only one deltaic body, which is the widest and thickest of the whole Bílina section. The deltaic bodies in sequence 3 are slightly thinner and show a gradual northward migration of the main locus of deposition. The deltaic strata of sequence 2, and of the northernmost part of sequence 3, were affected by growth faulting. Sequences 4 and 5 are traceable along the whole Bílina mine section, and thicken dramatically northwards (as in the case of sequence 3). The thinner parts of these sequences in the south are dominated by delta-plain palaeosols and large-scale channel fills. Northwards, thick deltaic bodies, largely deformed by growth faulting, appear and thicken. Sequence 6 is thin over the whole Bílina section, and is dominated by mouth

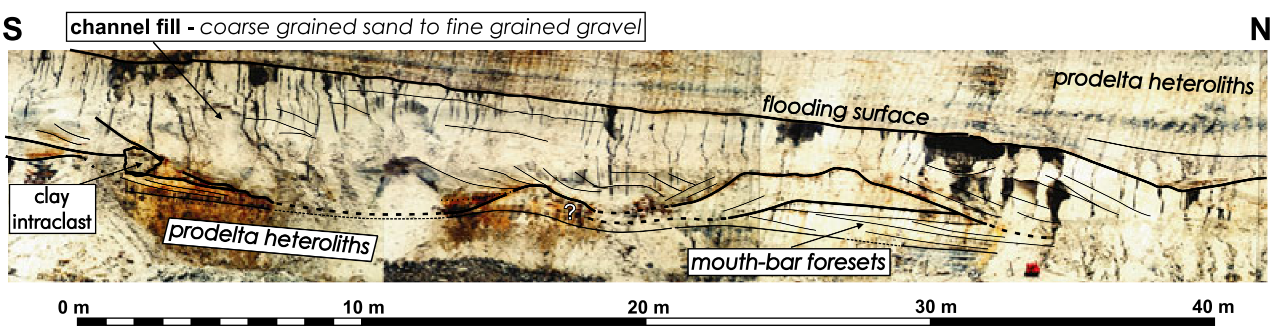

Fig. 17. Fluvial channel fills in the upper part of the delta complex (sequence 6) incised into mouth bar and prodelta deposits. Internal architecture of the channel suggests repeated base-level fluctuations. Locally, clay intraclasts up to 1 m in diameter occur on the channel floor. The youngest channel (upper right) is filled by transgressive lacustrine mud.

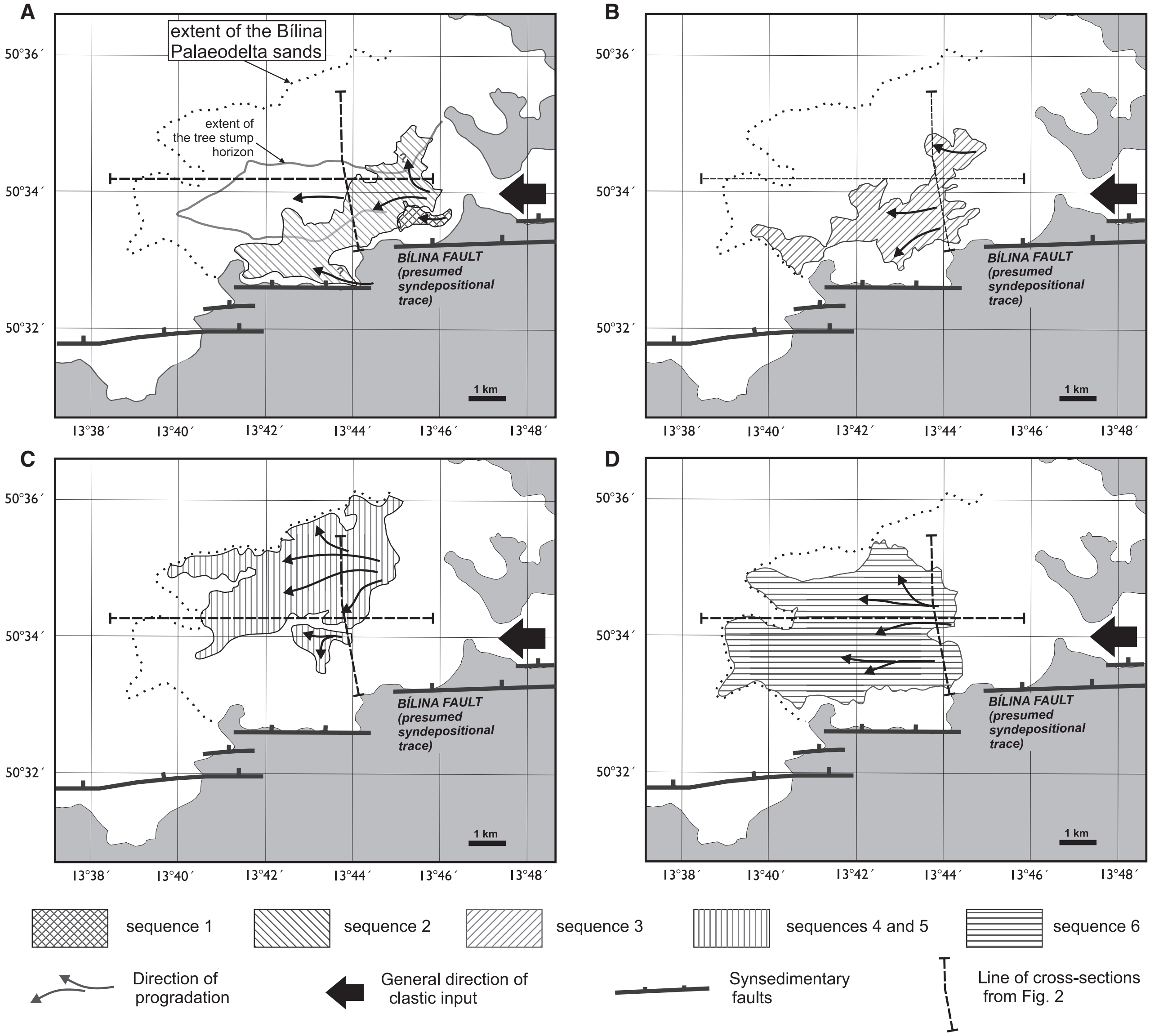

Fig. 18. Reconstruction of the areal extent of sandy equivalents of individual medium-term sequences distinguished within the Bílina Palaeodelta succession based on Mach (2003). (A) Areal extent of tree stump horizon above the lignite seam (grey line), and mouth-bar sands of medium-term sequences 1 and 2; (B) areal extent of mouth-bar sands of medium-term sequence 3; (C) areal extent of mouth-bar sands of medium-term sequences 4 and 5; (D) areal extent of mouth-bar sands of medium-term sequence 6.

bars with a high width to thickness ratio, thick palaeosols and large-scale channel fills. A specific feature of the uppermost part of this sequence is the retrogradation of a set of mouth-bar wedges towards the Bílina Fault. This retrogradational package forms a relatively thick (*ca* 20 m) TST, and the maximum transgressive surface covering this package terminates the Bílina deltaic succession. It is overlain by the Libkovice Member, interpreted as being fully lacustrine in this part of the basin (Malkovský *et al.*, 1985). According to Rajchl (2006), the drowning of the deltaic system was caused by subsidence along larger fault segments which formed during the second phase of extension.

Note that sequences 5 and 6 are only exposed in two dimensions, perpendicular to the general depositional dip. It is possible that additional medium-scale sequences are amalgamated in the complex of palaeosols, channel fills and thin mouth bars. The bulk of these sequences would have been deposited further basinwards, to the west of the Bílina region, with the study area largely bypassed by sediments. During high lake

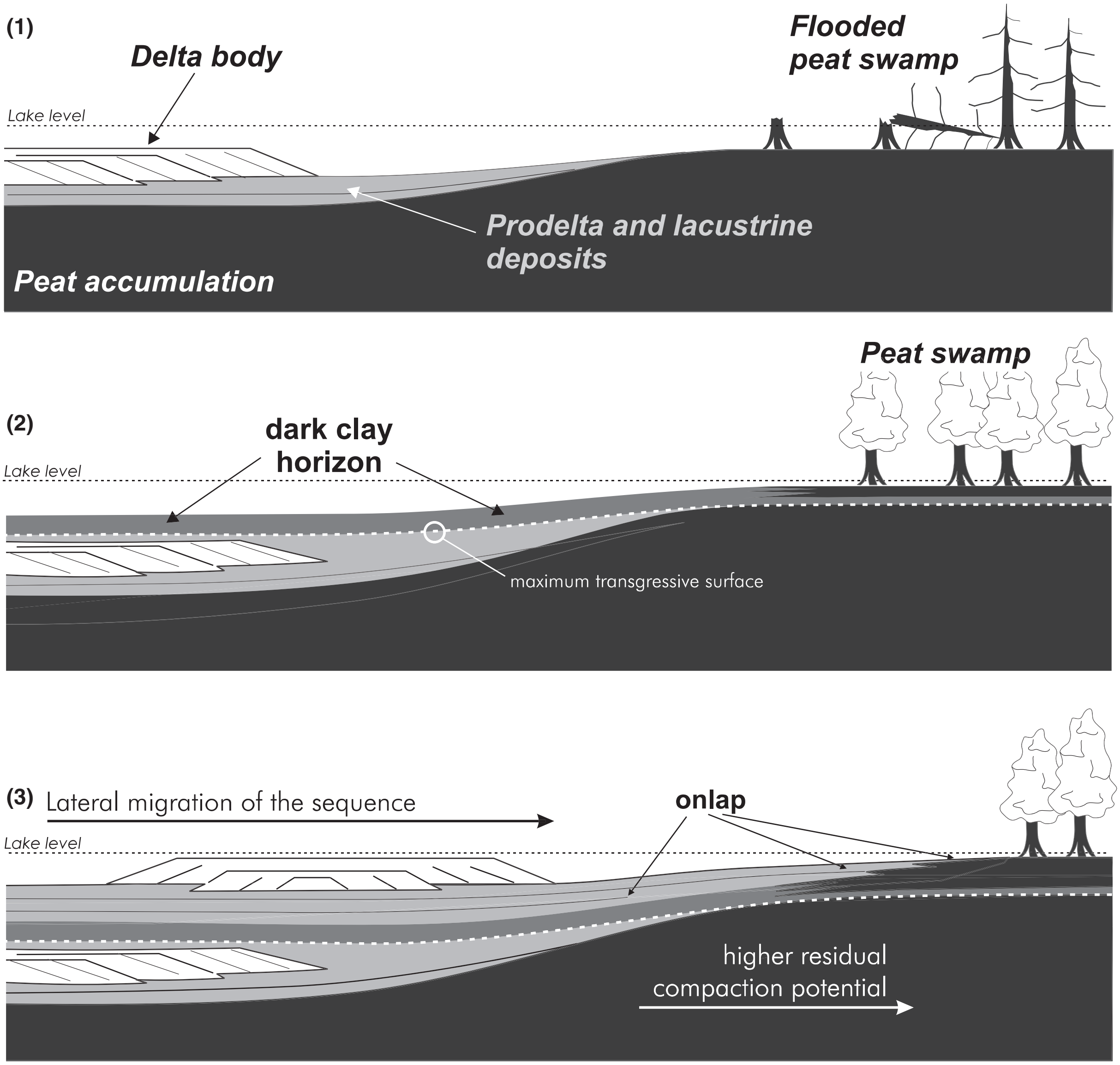

Fig. 19. A simplified model of flooding of the peat swamp surrounding the delta and lacustrine environment, and formation of prominent interbeds within the topmost part of the lignite seam. General direction of delta progradation is away from the viewer. Step 1: Increase in lake level, resulting in flooding of the peat swamp and retreat of the delta bodies. Step 2: Restoration of the peat swamp after filling of accommodation. Step 3: Migration of the deltaic sequence towards the location with higher residual compaction potential and the resulting gradual onlap onto the surface of the peat swamp.

levels, lacustrine facies did not reach this part of the delta plain and, instead, carbonaceous delta plain mud, interbedded with the palaeosols, may represent the proximal expression of maximum transgressive intervals.

Large-scale architecture: long-term sequence set

The base of the Bílina succession is marked by the contact of lacustrine clays of sequence 1 with the underlying lignite and palaeosols of the tree stump horizon shown in Figs 14 and 20. The fluvial system that began to deposit fine-grained clastics over a part of the peat swamp, was sourced from the east, in a way similar to that of the entire Bílina delta. The fact that it did not continue to develop as a fluvial system enclosed in the peat swamp (as described by Rajchl & Uličný, 2005), and instead was replaced by lacustrine and deltaic deposition, indicates a rapid increase in accommodation that could not be compensated by clastic and organic aggradation.

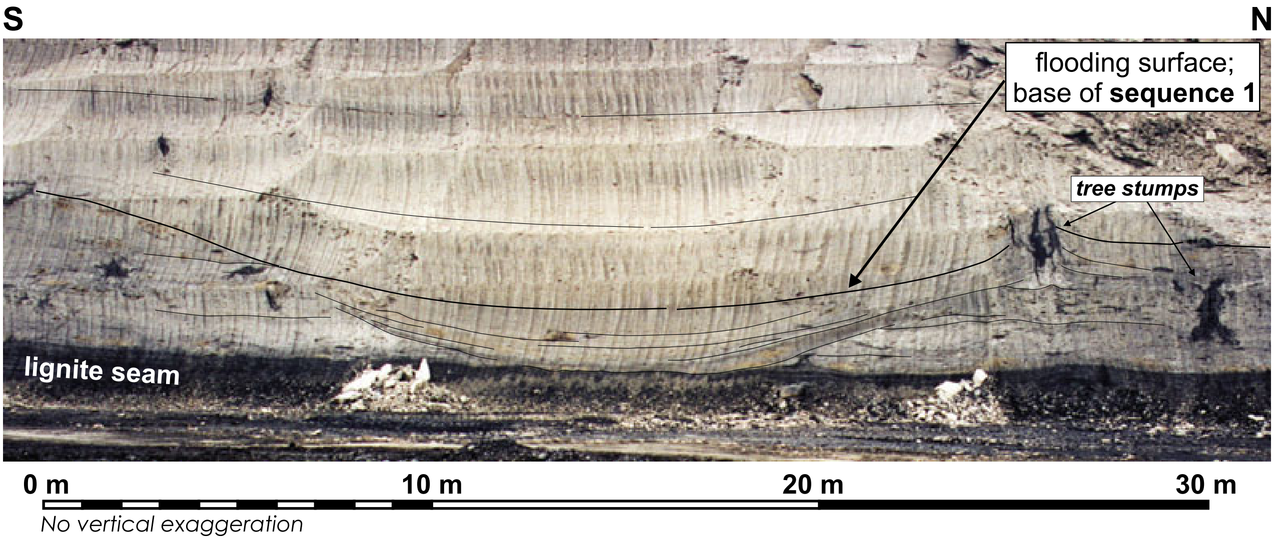

Fig. 20. Partly channellized interval of the lowest part of sequence 1. The channel fill is mud-dominated and is incised into a prominent tree stump horizon above the top of the main seam. Architecture of the channel fill suggests polyphase filling.

The overall succession from sequence 1 up to the middle of sequence 6 generally shows a long-term regressive trend accompanied by the migration of the depocentre to the north (Fig. 2A). The succession of Gilbert-type mouth bars, arranged in a retrogradational stacking pattern at the top of sequence 6, could be interpreted as a low-frequency transgressive sequence set on the scale of the overall Bílina succession. Thus, the whole Bílina deltaic succession represents a long-term sequence deposited between two flooding events: the initial flooding of the peat swamp and the drowning of the delta marked by gradual onlap of the lacustrine Libkovice Member (Fig. 2A).

CONTROLS ON THE BÍLINA PALAEODELTA DEPOSITION

The general controls that may have influenced the depositional history and architecture of the Bílina Palaeodelta include the following: (i) tectonics; (ii) climatically induced lake-level changes; and (iii) sediment loading, compaction and growth faulting. The interpreted relative roles of these controls and their typical depositional record are summarized in Fig. 21 and discussed below.

Tectonic versus climatic controls on accommodation

Tectonic subsidence caused by regional extension obviously controlled the formation of the Bílina Palaeodelta depocentre, but the limited extent of exposures, younger reactivation of bounding faults and post-depositional erosion make it difficult to identify a role for specific faults or to constrain the timing of displacement. However, synsedimentary tilting did affect part of the deltaic succession close to the Bílina Fault (Fig. 12). As documented below, the evolution of this fault influenced accommodation and the resulting stratal geometries.

Deltaic clastics of the Bílina succession and the underlying seam are tilted basinwards in a zone extending *ca* 900 m to the north of the Bílina Fault, i.e. away from the fault and roughly parallel to the dip of the sub-seam units (Fig. 2A). However, fanning of the dip angle between the underlying units (Cretaceous to Oligocene volcanics), the lignite seam and individual Bílina delta sequences suggest a synsedimentary origin for the tilt. The general dip angle of the seam top in the cross-section shown in Fig. 2A, which is roughly the true dip, reaches *ca* 18°, locally exceeding 20° but, within the overlying package of the medium-term sequences, a gradual upward decrease in the dip angle (to *ca* 7°) is observed.

A succession of mouth bars and prodelta to lacustrine deposits *ca* 150 m north of the exposed trace of the Bílina Fault is shown in Fig. 12. Using the mouth-bar topsets as a rough palaeohorizontal datum, basinward tilting of *ca* 10° is estimated to have occurred prior to the deposition of the mouth-bar complex (2) in Figure 12. In addition, the geometry of this mouth-bar complex shows backtilting due to the activity of small growth faults. The upward decrease in the dip angle

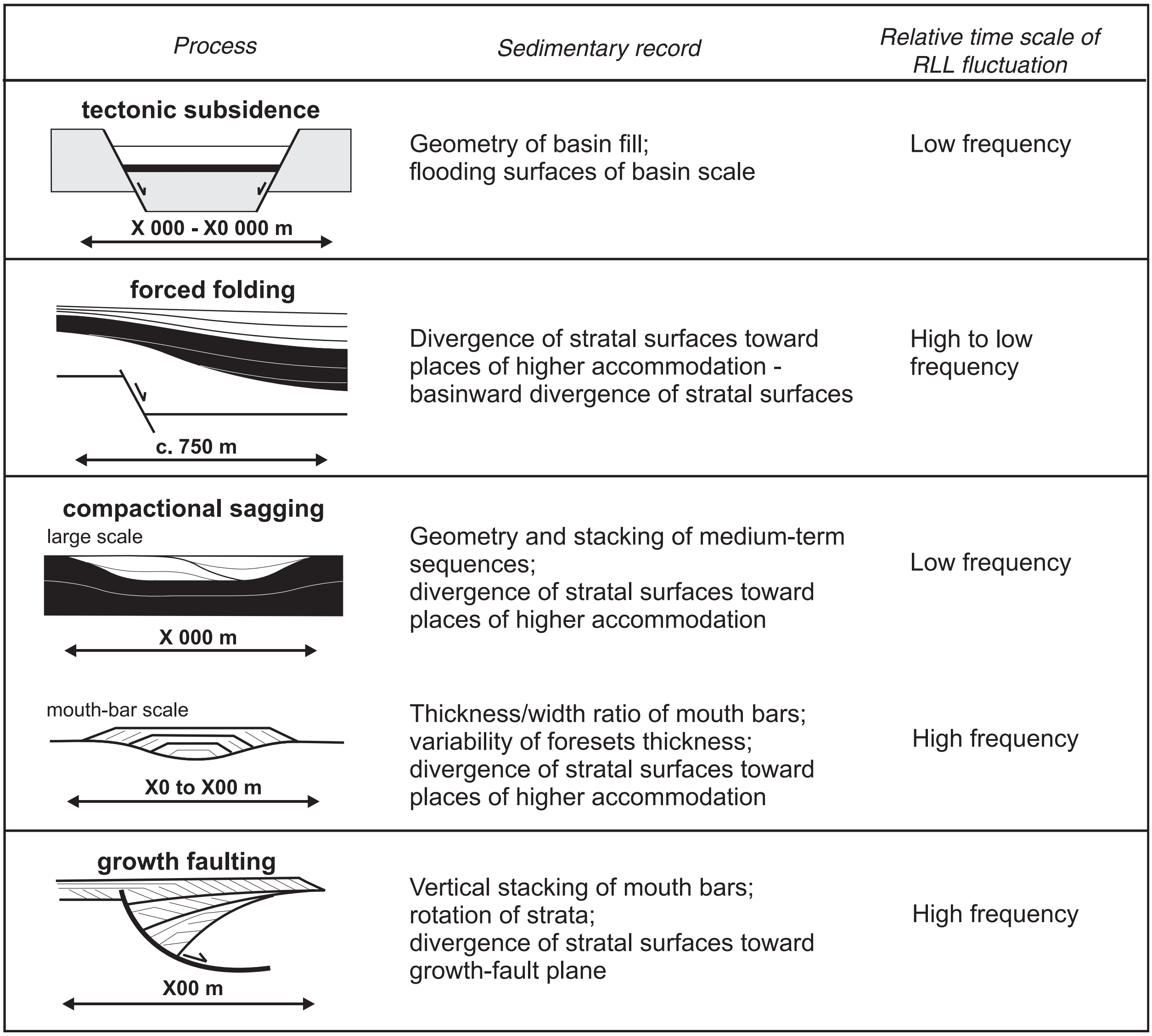

Fig. 21. Overview of the accommodation controls interpreted as having affected the architecture of the Bílina deltaic succession.

results in a basinward divergence of strata that cannot be explained by post-depositional fault drag. Instead, it is interpreted as caused by gradual synsedimentary tilting of the depositional surface due to forced folding above the upward-propagating Bílina Fault (cf. Gawthorpe *et al.*,1997; Gupta *et al.*, 1999; Jackson *et al.*, 2005, for similar cases). Growth faults, such as those shown in Fig. 12, are explained by gravity sliding (*sensu* Morley & Guerin, 1996) caused by synsedimentary tilting (see the following section for further details of the growth faults).

In general, the stratal architecture in the immediate vicinity of the Bílina Fault reflects a basinward increase in accommodation caused by the forced folding and provides evidence for syn-depositional propagation of the Bílina Fault segment towards the surface. Above sequence 5, further basinward divergence of strata is not observed. It is therefore inferred that the Bílina Fault segment reached the surface at this time and caused the onset of hangingwall subsidence in this location.

The widespread flooding surfaces that separate the lacustrine-deltaic succession from the underlying lignite seam and the overlying lacustrine strata, and those that subdivide the deltaic succession into medium-term sequences, are interpreted as indirect evidence for pulsed syn-depositional fault-related subsidence, rather than discharge fluctuations or climate-driven lake-level changes. The possibility of a climatic origin for the medium-term transgressive events (caused by discharge fluctuations) is inconsistent with the presumed hydrologically open character of the lake into which the Bílina Palaeodelta was built. The peat swamp may have been flooded temporarily, e.g. during seasonal high-discharge events. However, such floods probably did not result in flooding of the active mouth bars because the periods of high discharge would have been linked to higher sediment supply and hence continued progradation.

Climatically induced changes in accommodation are possibly indicated only in the case of minor forced regressions, documented above by the short-term offlaps such as that shown in Fig. 9. Overall, the small-scale sequences of the Bílina Palaeodelta reveal that the depositional setting was characterized by relatively high rates of accommodation creation which suppressed any tendency for significant relative lake-level falls. Theoretically, it is possible that the genetic sequences may have been controlled by fluctuations in sediment supply superimposed on a long-term, steady subsidence; however, changes in supply from the hinterland are difficult to prove and it is unlikely that the pattern of subsidence was steady, given the evidence for active faults. Liquefaction-induced deformation of deltaic deposits was reported by Rajchl & Uličný (2000b) and Uličný *et al.* (2000). A further control on accommodation could have been a change in elevation of the lake outlet but there is no evidence for this.

On balance, given the evidence for the syn-depositional displacements on the Bílina Fault, pulsed relative lake-level rises were probably caused by periods of increased subsidence (cf. Dorsey *et al.*, 1997) and this produced the flooding surfaces that are traceable throughout the clastic system and into the top of the lignite seam. The transition from the early fluvial system that transported clastics into the swamp, producing the stump horizon below sequence 1 and the overlying lacustrine-deltaic system, would have required an abrupt increase in accommodation, although not necessarily of large magnitude. An increase in tectonic subsidence rate near the end of the Bílina Palaeodelta deposition is interpreted from the retrogradational stacking of the youngest mouth bars of sequence 6. The final drowning, marked by deposition of the Libkovice Member clays (Fig. 1B), coincides with an increase in subsidence rate within the entire Eger Graben (cf. Špičáková *et al.*, 2000; Rajchl, 2006). So far, however, there is no conclusive evidence to relate this event to the change in extensional vectors interpreted by Rajchl (2006).

Compaction and growth faulting

The medium-term sequences 1 to 6 show lateral shifting of the depositional system through time (Fig. 16), as well as changes in their geometry and in the geometry of the internal architectural elements. The thinning and widening of progressively younger sequences resulted from gradual filling of accommodation by clastics, accompanied by the depletion of compaction potential of underlying peat. In particular, sequences 4 and 5 thicken markedly to the north, with sequence 4 onlapping the seam in the northernmost part of the Bílina mine (Fig. 16A). A reconstruction of the developing cross-sectional geometries of individual sequences exposed in the Bílina Mine is shown in Fig. 16B. The main mechanism that led to evolution of the geometries and successive migration of depocentres of the medium-term sequences is interpreted as follows: (i) the peat loaded by the deltaic and lacustrine clastics began to compact and sag and, thus, created additional accommodation (cf. Elliott, 1985; Courel, 1987; Rajchl *et al.*, 2002); (ii) with increasing filling of accommodation by clastics, and resulting compaction of the peat, the system began to migrate laterally towards locations of higher compaction potential – i.e. away from the previously deposited deltaic bodies which have already depleted the compaction potential of the underlying coal and clay (Fig. 16B). This mechanism is also documented by the upward-increasing percentage of thick delta-plain soils and large fluvial channel fills, at the expense of mouth bar and prodelta deposits, observed in the southern part of the section between sequences 4 and 6 (for details see Fig. 2A). These delta-plain deposits are interpreted as a record of condensed deposition resulting from deceleration of compaction-induced accommodation.

A possible role of forced folding in the lateral stacking of the medium-term sequences can be hypothesized only in the close vicinity of the Bílina Fault. However, the growing fault-propagation fold probably prevented a possible migration of the deltaic system southwards.

On the mouth-bar scale, the internal geometry of the mouth bars typically shows marked changes during deposition, which indicate local changes in accommodation (Figs 9B and 10). Compactional sagging (Fig. 9B) and growth faulting (Fig. 11) are interpreted as being the most important causes of the local variations in accommodation.

In the case of compactional sagging, local accommodation was created by loading of sandy mouth-bar deposits on prodelta and lacustrine sediments or peat (cf. Elliott, 1985; Courel, 1987). However, the increase in accommodation was not contemporaneous with sedimentation. Accommodation began to increase after a critical volume of sediment was deposited, as suggested by initial rapid progradation of foresets in the first stage of mouth-bar growth, followed by topset aggradation resulting from sagging which began subsequently (Figs 9 and 10A). The flooding surfaces separating individual progradational phases represent local drowning events related to episodes of non-deposition. The flooding surfaces tend to diverge towards areas of higher local accommodation (Fig. 9B).

The tendency towards sagging is positively correlated with the thickness of compactable substrate beneath the mouth-bar bodies. Upsection throughout the whole Bílina succession, a successive decrease in compaction potential of the substrate underlying the mouth bars is documented by the overall increasing width/thickness ratio of the mouth bars. For example, thin, laterally extensive mouth bars characterize the deltaic bodies in the uppermost part of the Bilina succession, underlain by a thick accumulation of heterolithic and sandy strata (Fig. 10B). On the contrary, vertically stacked and thick, laterally more localized mouth bars are typical of the delta bodies in the lower part of the Bilina succession (Fig. 9B), where they are underlain by thick lacustrine clays above the lignite seam.

In the majority of cases of growth faulting, the formation of a growth fault is triggered by loading of compactible substrate by a rapid input of coarse-grained sediments (Rajchl & Uličný, 2002) and by the mobility of thick underlying substrate (cf. Morley & Guerin, 1996). The role of downslope motions (gravity sliding) during creation of growth faults (*sensu* Morley & Guerin, 1996) is inferred only in the case of the growth faults close to the Bílina Fault, in the zone of interpreted fault-propagation folding (see above and Fig. 12). Unlike the other cases, here the mean dip azimuth of the growth faults generally corresponds with the dip of the Bílina Fault.

The presence of a growth fault resulted in: (i) a faster aggradation of topsets within a single mouth bar compared to the area beyond the growth fault block; (ii) divergence of hangingwall strata towards the growth fault plane; and (iii) vertical stacking of multiple mouth-bar bodies separated by localized flooding surfaces (Fig. 11). These effects reflect increased accommodation creation due to the presence of the growth faults (i) and (iii), rotation of the hangingwall (ii) and repeated episodes of incremental slip on the growth fault (iii). The uplift of the footwall antiform could have led to local relative lake-level fall (Fig. 11).

Whether topset aggradation or formation of a new mouth bar prevailed in the architecture on the hangingwall side depended on the ratio between the rates of hangingwall subsidence and sedimentation. During continued progradation of an individual mouth bar the increments of accommodation were insignificant or were compensated for by aggradation of the topsets. Drowning of the older mouth bar and the creation of space for a new mouth bar occurred during episodes of non-deposition that may have resulted from local fluctuations in sediment supply. These fluctuations may have also driven or, at least, influenced the incremental slip on the growth fault (cf. Morley & Guerin, 1996; Mauduit *et al.*, 1997).

As in the case of the compactional sags, the development of growth faults generally depended on the presence of a sufficient thickness of compactible substrate (lacustrine deposits and/or peat) underlying the deltaic deposits. The tendency to growth faulting increased with the increasing thickness of the compactible substrate (see Fig. 2A and C).

Although a significant role for compaction is documented above for the creation of accommodation, it could not have been the main trigger that caused extensive transgressive episodes that separate medium-term sequences. Effects of medium-term transgressions are correlated across the whole deltaic system and the peat swamp, but a relative lake-level rise caused by compaction would affect only the loaded area. On the other hand, compaction of the peat and, to some extent, of the lacustrine clays, significantly added to the primary accommodation of tectonic origin. Compaction and growth faulting are interpreted as the most important causes of local increased accommodation at the scale of the short-term sequences.

CONCLUSIONS

The Bílina example shows that, in an extensional basin with a thick peat accumulation, tectonics and compaction can have comparable effects on stratal geometries on various temporal and spatial scales. However, the quality and size of the exposures, together with the geological context, allow tectonic and compactional effects to be distinguished (cf. Fig. 21).

An increased rate of tectonic subsidence in the receiving graben is interpreted as having caused both the onset and termination of deltaic sedimentation in the Bílina area. The transgressive-regressive history of the medium-term sequences (deltaic lobes with corresponding lacustrine strata) was probably driven by episodes of increased subsidence rate, but the stratal architecture of the sequences was strongly affected by compaction of underlying peat and clay. Compaction controlled both the width and thickness of these sequences, and the lateral migration of the locus of clastic deposition. The only exception is observed in the close vicinity of the Bílina Fault, where fault-propagation folding is interpreted as having affected the stratal geometry during part of the delta evolution. At short time scales, the effects of compaction are most pronounced in the geometries of individual mouth bars and groups of mouth bars (short-term sequences). The interaction among sediment loading, compaction and growth faulting controlled the high-frequency relative lake-level fluctuations which defined the short-term sequences.

ACKNOWLEDGEMENTS

Financial support to M. Rajchl and D. Uličný was provided by the Government of the Czech Republic through GAČR (Czech Science Foundation) grant 205/01/0629. MR was partially supported by the MZP0002579801 research programme of the Ministry of Environment of the Czech Republic. DU was supported by the Czech Academy of Sciences research programme AV0Z30120515 during the course of this research. Acquisition of reprocessed seismic reflection data was made possible by the Ministry of Environment of the Czech Republic, contract no. OG 13/02. K. Mach thanks the Severočeské doly a.s., for support, and MR and DU thank the company for granting access to the Bílina Mine. The authors thank Guy Plint for a detailed review of the first draft of the manuscript, and are grateful to J. Aitken, R. Flores and, in particular, P. Haughton for their thorough reviews and constructive comments. However, the responsibility for any possible omissions and misinterpretations remains with the authors.

REFERENCES

Adamovič, J. and **Coubal, M.** (1999) Intrusive geometries and Cenozoic stress history of the northern part of the Bohemian Massif. *Geolines*, **9**, 5–14.

Allen, P.A. (1997) *Earth Surface Processes*. Blackwell, Oxford. 247 pp.

Bhattacharya, J.P. and **Walker, R.G.** (1992) Deltas. In: *Facies Models* (Eds R.G. Walker and N.P. James), 2nd edn, pp. 157–177. Geological Association of Canada, St. John's.

Bridge, J.S. (1993) Description and interpretation of fluvial deposits: a critical perspective. *Sedimentology*, **40**, 801–810.

Bridge, J.S. (2003) *Rivers and Floodplains: Forms, Processes, and Sedimentary Record*. Blackwell, Oxford, 491 pp.

Cajz, V. (2000) Proposal of lithostratigraphy for the České středohoří Mts. volcanics. *Bull. Czech Geol. Surv.*, **75**, 7–16.

Cajz, V., **Vokurka, K.**, **Balogh, K.**, **Lang, M.** and **Ulrych, J.** (1999) The České středohoří Mts. volkanistratigraphy and geochemistry. *Geolines*, **9**, 21–28.

Courel, L. (1987) Stages in the compaction of peat; examples from the Stephanian and Permian of the Massif Central, France. *J. Geol. Soc.*, **144**, 489–493.

Čtyroký, P. and **Witt, W.** (1998) Lower Miocene freshwater ostracods and gastropods from the Chomutov area of Northern Bohemia, Czech Republic. *Věst. Čes. Geol. Úst.*, **73**, 281–285.

Diessel, C.F.K. (1992) *Coal-Bearing. Depositional Systems*. Springer-Verlag, Berlin, pp. 330–336

Dorsey, R.J., **Umhoefer, P.J.** and **Falk, P.** (1997) Earthquake clustering inferred from Pliocene Gilbert-type fan deltas in the Loreto basin, Baja California Sur, Mexico. *Geology*, **25**, 679–682.

Dvořák, Z. and **Mach, K.** (1999) Deltaic deposits in the North-Bohemian Brown Coal Basin and their documentation in the Bílina opencast mine. *Acta Univ. Carol.-Geologica*, **43**, 633–641.

Edwards, M.B. (1976) Growth faulting in Upper Triassic deltaic sediments, Svalbard. *AAPG Bull.*, **60**, 341–355.

Elliott, R.E. (1985) Quantification of peat to coal compaction stages, based especially on phenomena in the East Pennine Coalfield, England. *Proc. Yorks. Geol. Soc.*, **45**, 163–172.

Flint, S., **Stewart, D.J.** and **van Riessen, E.D.** (1989) Reservoir geology of the Sirikit oilfield, Thailand: lacustrine deltaic sedimentation in a Tertiary intermontane basin. In: *Deltas: Sites and Traps for Fossil Fuels* (Eds M.K.G. Whateley and K.T. Pickering), *Geological Society Spec. Publ.*, **41**, 223–237.

Flores, R.M. (1990) Transverse and longitudinal Gilbert-type deltas, Tertiary Coalmont Formation, North Park Basin, Colorado, USA. In: *Coarse-Grained Deltas* (Eds A. Collela and D.B. Prior), *IAS Spec. Publ.*, **10**, 223–233.

Flores, R.M. and **Pillmore, C.L.** (1987) Tectonic control on alluvial paleoarchitecture of the Cretaceous and tertiary Raton basin, Colorado and New Mexico. In: *Recent Developments in Fluvial Sedimentology* (Eds F.G. Ethridge, R.M. Flores and M.D. Harvey), *SEPM Spec. Publ.*, **39**, 311–320.

Frazier, D.E. (1967) Recent deltaic deposits of the Mississippi delta: their development and chronology. *Trans. Gulf Coast Assoc. Geol. Soc.*, **17**, 287–315.

Galloway, W.E. (1989) Genetic stratigraphic sequences in basin analysis .1. Architecture and genesis of flooding-surface bounded depositional units. *AAPG Bull.*, **73**, 125–142.

Gawthorpe, R.L., Fraser, A.J. and **Collier, R.E.L.** (1994) Sequence stratigraphy in active extensional basins: implications for the interpretation of ancient basin-fills. *Mar. Petrol. Geol.*, **11**, 642–658.

Gawthorpe, R.L., Sharp, I., Unerhill, J.R. and **Gupta, S.** (1997) Linked sequence stratigraphic and structural evolution of propagating normal faults. *Geology*, **25**, 795–798.

Gay, S.P. (1989) Gravitational compaction, a neglected mechanism in structural and stratigraphic studies: new evidence from Mid-Continent, USA. *AAPG Bull.*, **73**, 641–657.

Gradstein, F.M., Ogg, J.G. and **Smith, A.G.** (2004) *A Geologic Time Scale 2004.* Cambridge University Press, Cambridge.

Gupta, S., Underhill, J.R., Sharp, I.R. and **Gawthorpe, R.L.** (1999) Role of fault interactions in controlling synrift sediment dispersal patterns: Miocene, Abu Alaqua Group, Suez Rift, Sinai, Egypt. *Basin Res.*, **11**, 167–189.

Helland-Hansen, W. and **Martinsen, O.J.** (1996) Shoreline trajectories and sequences: description of variable depositional-dip scenarios. *J. Sed. Res.*, **66**, 670–689.

Howell, J.A., Flint, S.S. and **Hunt, C.** (1996) Sedimentological aspects of the Humber Group (Upper Jurassic) of the South Central Graben, UK North Sea. *Sedimentology*, **43**, 89–114.

Hunt, D., Allsop, T. and **Swarbrick, R.E.** (1996) Compaction as a primary control on the architecture and development of depositional sequences: conceptual framework, applications and implications. In: *High Resolution Sequence Stratigraphy: Innovations and Applications* (Eds J.A. Howell and J.F. Aitken), *Geol. Soc. Spec. Publ.*, **104**, 21–345.

Hurník, S. (1959) Prvé zjištění cyklické sedimentace v terciérních limnických pánvích ČSR. *Věstník ÚÚG*, **34**, 269–278.

Jackson, C.A.L., Gawthorpe, R.L., Carr, I.D. and **Sharp, I.R.** (2005) Normal faulting as a control on the stratigraphic development of shallow marine syn-rift sequences: the Nukhul and Lower Rudeis Formations, Hammam Faraun fault block, Suez Rift, Egypt. *Sedimentology*, **52**, 313–338.

Jihlavec, F. and **Novák, J.** (1986) Reflexně seismická měření v severočeské pánvi. *Geologický průzkum*, **5/1986**, 136–138.

Jopling, A.V. (1965) Hydraulic factors controlling the shape of laminae in laboratory deltas. *J. Sed. Petrol.*, **35**, 777–791.

Kostic, S., Parker, G. and **Marr, J.G.** (2002) Role of turbidity currents in setting the foreset slope of clinoforms prograding into standing fresh water. *J. Sed. Res.*, **72**, 353–362.

Kvaček, Z. (1998) Bílina: a window on Early Miocene marshland environments. *Rev. Palaeobot. Palynol.*, **101**, 111–123.

Kvaček, Z., Böhme, M., Dvořák, Z., Konzalová, M., Mach, K., Prokop, J. and **Rajchl, M.** (2004) Early Miocene freshwater and swamp ecosystems of the Most Basin (northern Bohemia) with particular reference to the Bílina Mine section. *J. Czech Geol. Soc.* **49/1–2,** 1–40.

Mach, K. (1997) A logging correlation scheme for the main coal seam of the North Bohemian brown coal basin, and the implications for the palaeogeographical development of the basin. In: *European Coal Geology and Technology* (Eds R. Gayer and J. Pešek), *Geol. Soc. Spec. Publ.*, **125**, 309–320.

Mach, K. (2002) Genesis of large scale syndepositional deformations of main coal seam – Miocene Bílina delta, Most basin, Czech Republic. Programme and abstracts of 5th European Coal Conference, 90. Mons-Frameries, Belgium.

Mach, K. (2003) Anomální stavba hlavní hnědouhelné sloje v prostoru miocenní bílinské delty a její geneze. PhD Thesis, Charles University, Prague.

Mach, K., Žák, K. and **Jačková, I.** (1999) Zastoupení a izotopové složení jednotlivých forem síry ve vertikálním profilu hlavní uhelné sloje v severočeské hnědouhelné pánvi a jejich paleogeografický význam. *Věstník ČGÚ*, **74**, 51–66.

Malkovský, M. (1995) Některé problémy chronostratigrafického členění terciéru Českého masivu. In: *Nové výsledky v terciéru Západních Karpat II* (Sborník referátů z 11. konference o mladším terciéru), (Ed. B. Hamršmíd), pp. 25–36. MND, Hodonín, Czech Republic.

Malkovský, M. *et al.* (1985) *Geologie severočeské hnědouhelné pánve a jejího okolí.* ÚÚG Academia, Praha.

Massari, F. (1996) Upper-flow-regime stratification types on steep-face, coarse-grained, Gilbert-type wedges (Pleistocene, Southern Italy). *J. Sed. Res.*, **66**, 364–375.

Mauduit, T., Guerin, G., Brun, J.-P. and **Lecuna, H.** (1997) Raft tectonics: the effects of basal slope angle and sedimentation rate on progressive extension. *J. Sed. Geol.*, **19**, 1219–1230.

Miall, A.D. (1985) Architectural-element analysis – a new method of facies analysis applied to fluvial deposits. *Earth-Sci. Rev.*, **22**, 261–308.

Miall, A.D. (1988) Architectural elements and bounding surfaces in fluvial deposits: anatomy of the Rayenta Formation (Lower Jurassic), Southwest Colorado. *Sed. Geol.*, **55**, 233–262.

Miall, A.D. (1991) Stratigraphic sequences and their chronostratigraphic correlation. *J. Sed. Petrol.*, **61**, 497–505.

Miall, A.D. (1996) *The Geology of Fluvial Deposits*. Springer-Verlag, New York.

Michaelsen, P., Henderson, R.A., Crosdale, P.J. and **Mikkelsen, S.O.** (2000) Facies architecture and depositional dynamics of the Upper Permian Rangal Coal Measures, Bowen Basin, Australia. *J. Sed. Res.*, **70**, 879–895.

Morley, C.K. and **Guerin, G.** (1996) Comparison of gravity-driven deformation styles and behaviour associated with mobile shales and salt. *Tectonics*, **15**, 1154–1170.

Nadon, G.C. (1998) Magnitude and timing of peat-to-coal compaction. *Geology*, **26**, 727–730.

Nemec, W. (1990) Aspects of sediment movement on steep delta slope. In: *Coarse-Grained Deltas* (Eds A. Collela and D.B. Prior), *IAS Spec. Publ.*, **10**, 29–75.

Nemec, W., Steel, J., Gjelberg, J., Collinson, J.D., Prestholm, E. and **Øxnevad, I.E.** (1988) Anatomy of collapsed and re-established delta front in Lower Cretaceous of Eastern Spitsbergen: gravitational sliding and sedimentation processes. *AAPG Bull.*, **72**, 454–476.

Peacock, D.C.P. and **Sanderson, D.J.** (1994) Geometry and development of relay ramps in normal fault systems. *AAPG Bull.*, **78**, 147–165.

Postma, G. (1990) Depositional architecture and facies of river and fan deltas: a synthesis. In: *Coarse-Grained Deltas* (Eds A. Collela and D.B. Prior), *IAS Spec. Publ.*, **10**, 13–27.

Postma, G. (1995) Sea-level-related architectural trends in coarse-grained delta complexes. *Sed. Geol.*, **98**, 3–12.

Rajchl, M., Uličný, D. and **Hubatka, F.** (2003a) Syn- and post-sedimentary tectonics of the Most Basin (Ohře Rift, Czech Republic); insights from reflection-seismic data. Proceedings of the 8th Meeting of the Czech Tectonic Studies Group. *Geolines*, **16**, 86.

Rajchl, M., Uličný, D., Mach, K. and **Hubatka, F.** (2003b) Large-scale stratigraphic geometries in a rift-margin, lacustrine delta system influenced by peat compaction: comparison of field and reflection seismic data (The Miocene Bílina Delta, Ohře Rift, Czech Republic). Proceedings of the 5th Meeting of the Czech Tectonic Studies Group. *Geolines*, **16**, 87.

Rajchl, M. (1999) Structures due to synsedimentary deformation in sediments of the Bílina Delta (Miocene, Most Basin, Czech Republic). Proceedings of the 4th Meeting of the Czech tectonic Studies Group. *Geolines*, **8,** 57.

Rajchl, M. (2006) Tectonosedimentary evolution and fluviodeltaic systems of the Most Basin (Tertiary, Eger Graben, Czech Republic). PhD Thesis, Charles University, Prague.

Rajchl, M. and **Uličný, D**. (1999) Sedimentární model bílinské delty. *Zpravodaj Hnědé uhlí*, 15–42 (The Depositional Model of the Bílina Delta; in Czech with English summary).

Rajchl, M. and **Uličný, D.** (2000a) Evolution of basin-fill geometries in the Most Basin: implications for the tectonosedimentary history of the Ohře Rift (Eger Graben), North Bohemia. Proceedings of the 5th Meeting of the Czech Tectonic Studies Group. *Geolines*, **10,** 62–63.

Rajchl, M. and **Uličný, D**. (2000b). *Drobné synsedimentární deformační struktury v klastických sedimentech bílinské delty (Miocén, mostecká pánev). Zpravodaj Hnědé Uhlí*, **3/2000,** 29–41 (Small-scale soft-sediment deformation structures in the classic deposits of the Bílina Delta – Miocene, Most Basin; in Czech with English summary).

Rajchl, M. and **Uličný, D.** (2002) Architecture of Deltaic Bodies Affected by Growth Faulting: Examples from the Bílina Delta (Neogene, Most Basin, Czech Republic). VII. Česká tektonická skupina, Zelazno – Poland, 9.–12.5. 2002. *Geolines*, **14,** 78.

Rajchl, M. and **Uličný, D.** (2005) Depositional record of an avulsive fluvial system controlled by peat compaction (Neogene, Most Basin, Czech Republic). *Sedimentology*, **52,** 601–625.

Rajchl, M., Uličný, D. and **Mach, K**. (2002) *Stratigraphic Geometries and Sequences in a Rift-Margin, Lacustrine Delta System Influenced by Peat Compaction: The Miocene Bilina Delta, Eger Graben, Czech Republic.* Abstract Volume of 16th IAS International Sedimentological Congress, Rand Afrikaans University, Johannesburg, South Africa.

Reynolds, D.J., Steckler, M.S. and **Coakley, B.J.** (1991) The role of the sediment load in sequence stratigraphy; the influence of flexural isostasy and compaction. *J. Geophys. Res.*, **96,** 6931–6949.

Ryer, T.A. and **Langer, A.W.** (1980) Thickness change involved in the peat-to-coal transformation for a bituminous coal of Cretaceous age in Central Utah. *J. Sed. Petrol.*, **50,** 0987–0992.

Shrbený, O., Bůžek, Č., Čtyroký, P., Fejfar, O., Konzalová, M., Kvaček, Z., Malecha, A., Šantrůček, P. and **Václ, J.** (1994) Terciér českého masívu. In: *Geologický atlas České republiky stratigrafie* (Ed J. Klomínský), Sheet 3. ČGÚ, Praha.

Špičáková, L., Uličný, D. and **Koudelková, G.** (2000) Tectonosedimentary evolution of the Cheb Basin (NW Bohemia, Czech Republic) between Late Oligocene and Pliocene: a preliminary note. *Studia Geophys. Geodaet.*, **44,** 556–580.

Suhr, P. (2003) The Bohemian Massif as a catchment area for the NW European Tertiary Basin. Proceedings of Symposium Hibsch 2002. *Geolines*, **15,** 147–160.

Swift, D.J.P., Phillips, S. and **Thorne, J.A.** (1991) Sedimentation on continental margins; V, parasequences. In: *Shelf Sand and Sandstone Bodies: Geometry, Facies and Sequence Stratigraphy* (Eds D.J.P. Swift, G.F. Oertel, R.W. Tillman and J.A. Thorne), *Int. Assoc. Sedimentol. Spec. Publ.*, **14,** 153–187.

Sýkorová, I., Černý, J., Pavlíková, H. and **Weishauptová, Z**. (1997) Composition and properties of North Bohemian coals. In: *European Coal Geology and Technology* (Eds R. Gayer and J. Pešek), *Geol. Soc. Spec. Publ.* **125,** 207–217.

Törnqvist, T.E., Kidder, T.R. and **Autin, W.J.** (1996) A revised chronology for Mississippi River subdeltas. *Science*, **273,** 1693–1696.

Uličný, D., Rajchl, M., Mach, K. and **Dvořák, Z.** (2000) Sedimentation and synsedimentary deformation in a rift-margin, lacustrine delta system: the Bílina Delta (Miocene), Most Basin. Proceedings of the 5th Meeting of the Czech tectonic Studies Group. *Geolines*, **10,** 84–95.

Van Heerden, I.L. and **Roberts, H.H.** (1988) Facies development of Atchafalaya Delta, Louisiana: a modern bayhead delta. *AAPG Bull.*, **72,** 439–453.

Van Wagoner, J.C., Posamentier, H.W., Mitchum, R.M., Vail, P.R., Sarg, J.F., Loutit, T.S. and **Hardenbol, J**. (1988) An overview of fundamentals of sequence stratigraphy and key definitions. In: *Sea-Level Changes: An Integrated Approach* (ed. C.K. Wilgus), *Soc. Econ. Palaeont. Mineral. Spec. Publ.*, **42,** 39–44.

Van Wagoner, J.C., Mitchum, R.M., Campion, K.M. and **Rahmanian, V.D.** (1990) Siliciclastic sequence stratigraphy in well logs, cores, and outcrops. *AAPG Meth. Explor. Ser.*, **7,** 1–55.

Wright, L.D. (1977) Sediment transport and deposition at river mouth: a synthesis. *Bull. Geol. Soc. Am.*, **88,** 857–868.

Manuscript received 12 August 2004; revision accepted 6 December 2007